ELECTRONIC SYSTEMS DIVISION

LASA SIGNAL PROCESSING, SIMULATION, AND COMMUNICATIONS STUDY

Second Quarterly Technical Report

MAY - AUGUST 1966

DEPUTY FOR ADVANCED PLANNING
ELECTRONIC SYSTEMS DIVISION
AIR FORCE SYSTEMS COMMAND
United States Air Force
L. G. Hanscom Field, Bedford, Massachusetts

Distribution of this document is unlimited.

Sponsored by:

Advanced Research Projects Agency
Washington, D. C.

ARPA Order No. 800

(Prepared under Contract No. AF 19(628)-5948 by International Business Machines Corporation, 18100 Frederick Pike, Gaithersburg, Maryland 20760)

LASA
SIGNAL PROCESSING, SIMULATION, AND COMMUNICATIONS STUDY

Second Quarterly Technical Report

MAY - AUGUST 1966

DEPUTY FOR ADVANCED PLANNING
ELECTRONIC SYSTEMS DIVISION
AIR FORCE SYSTEMS COMMAND
United States Air Force
L. G. Hanscom Field, Bedford, Massachusetts

Distribution of this document is unlimited.

Sponsored by:

Advanced Research Projects Agency
Washington, D. C.

ARPA Order No. 800

(Prepared under Contract No. AF 19(628)-5948 by International Business Machines Corporation, 18100 Frederick Pike, Gaithersburg, Maryland 20760)

ACKNOWLEDGMENT

This research was supported by the Advanced Research Projects Agency and was monitored by Electronic Systems Division under Contract Number AF 19(628)-5948.

SYNOPSIS

In the First Quarterly Technical Report, 14 May 1966, a functional system description of a LASA Signal Processing System was hypothesized. Certain system parameters were outlined and bounded to permit a definition of the signal processing concept. This, the Second Quarterly Technical Report, discusses important system parameters in greater detail to provide further technical support to the system concept and describes some of the supporting efforts.

Sections 1 and 2 describe the work accomplished and future plans. Appendices A to C contain factual detail in the areas of beam analysis, signal processing and processing systems. Appendix D describes effort relating to communications instrumentation. A summary description of the computer programs currently under development is given in Appendix E. Overall program comments and recommendations on relevant topics of seismological interest are presented in Appendix F.

CONTENTS

Section 1

WORK ACCOMPLISHED AND RESULTS OBTAINED

During this quarter, work supporting the overall system function described in the First Quarterly Technical Report* has been accomplished. The scaling requirements in the detection processing function have been detailed; process simulation programs have been prepared and limited amounts of data analyzed; gross system functions both internal and external to event and detection processing have been partitioned and further analyzed; and the experimental display has been constructed. The array study task has been assigned a low priority largely because of the desirability of testing, by means of the simulation programs and the display, the actual criticality of seismometer placement and the real importance of side-lobe reduction.

To facilitate the presentation of factual detail in this section, the following task summaries are organized according to the order delineated in the contract.

1.1 ARRAY STUDY

A new program for the calculation of beam patterns is in preparation. This program will facilitate array synthesis by making use of superposition of array elements and corresponding beam patterns. To accomplish this will require a capability to plot phase as well as logarithmic amplitude contours. This program may become useful for possible Montana LASA side-lobe reduction as well as further study of regular polygon arrays.

An important simulation result concerning subarray geometry is that, under most circumstances, subarray signal-to-noise ratio gain can be enhanced by not using the B-ring of six seismometers of the present subarrays, thus,

*IBM First Quarterly Technical Report, "LASA Signal Processing, Simulation and Communications Study," Contract No. AF 19(628)-5948, May 27, 1966.

decreasing the signal processing load. This result appears to be consistent with results of others who have found that it would be advantageous to increase the subarray diameter. It has also been found that one of the six subarray beams may be eliminated by dispersing the subarray centers. Results of studies pertaining to beam requirements are presented in Appendix A.

1.2 STEERING DELAY STUDY

Steering Delay Analysis programs have been modified and are ready to be applied to a significant number of LASA wave-front arrivals. Central to these programs is the Least Squares Wavefront program which has been amended so as to calculate best fitting quadratic wave fronts as well as plane fronts. In the event that the second order (curvature) parameters should contain a significant predictable component, this addition will be valuable for reducing the magnitude of the residuals. Other programs which are to be used in the Steering Delay Study are Seismic Steering Delay Anomalies, Ray Tracing, Inverse Velocity Space Mapping, and Cross-Covariance.

Limited experience to date in measuring delay anomalies as well as experience from analytical and processing simulation studies indicates that steering delay errors amounting to a beam loss of a few db at 1.5 Hz may be inherent in the use of the preformed beams for detection and routine event processing purposes. For this reason, a special processing function using event-tailored beams is intended for those detections of particular interest. Such detections will also include wave arrivals needed for updating system calibration.

1.3 PROCESSING REQUIREMENTS

A method of calculating signal scaling in the beamforming-filtering operation, so as to retain a sufficiently high saturation level while preventing excessive deterioration due to round-off error, has been developed and is presented in Appendix B.

A limited amount of simulation of subarray beamforming has been performed for the Longshot event with several types of filtering (see Appendix B). Thus, a method has been established to permit identification of those filters which achieve

maximum signal-to-noise ratio. Furthermore, an anticipated improvement in subarray signal-to-noise ratio obtained by dropping the B-ring of seismometers was substantiated by the simulation. This fact will lead to a modest saving of computational effort required to implement a signal processing system while generally increasing system performance.

It has been determined that the sampling losses associated with detection processing are acceptable if the subarray and LASA beamforming are executed at a rate of 10 and 5 Hz, respectively. The beamforming phase losses are reasonably contained if the subarray and LASA beamforming resolutions are 20 and 10 Hz, respectively. In this manner, the subarray beam bandpass filtering may be performed at 10 Hz and the pre-detection and detection processing of LASA beams may be executed at 5 Hz (Appendix B).

Algorithm specifications have been refined to permit more efficient microcoding, and each algorithm is being simulated in assembly language.

A working breadboard model of a beam display has been built, and is being used to evaluate its applicability in the system monitor function and to study beam formations, particularly for event processing.

Further consideration given to the problems of event processing appear to lead in the direction of two changes in emphasis. First, the likelihood that preformed beams will always be a few db below tailor-made beams, especially at the high frequencies, suggests the importance of a capability for special processing beyond that using preformed beams routinely generated in the event beamformer. Secondly, the probable existence of post-P arrivals and side-lobe detections for larger events requires a capability for the event processor to sort and identify many of these arrivals, leading to both logic requirements and additional beamforming capability outside the P-teleseismic zone.

Considerable work has been done in defining such operational system functions as monitor, maintenance, diagnostics, interface requirements, operation consoles, displays, and system reliability. Particular emphasis has been given to the repairable duplex system mode of operation to assure maximum system usability, especially in the detection processing and recording functions. The techniques employed in these processing system studies are presented in Appendix C.

1.4 COMMUNICATIONS

The activity in communications directed at the transmission of LASA data over existing common carrier systems has indicated the trade-offs possible in relating cost to word size, sampling rate and distance between the array and the signal processing system. A description of this work is included for the sake of completeness in Appendix D.

1.5 DATA ANALYSIS PROGRAMS

A number of programs have been written or adapted for purposes of data analysis and simulation. A brief description of their function and input-output requirements and capabilities is presented in Appendix E.

1.6 COMMENTS

The IBM LASA program has been reviewed from a seismological viewpoint by the project's seismology consultant. A summary of his comments is presented in Appendix F. He has, on the whole, found the approaches taken in developing the functional processing system to be reasonable and based on seismological facts as well as they are known at this time. He has also expressed an interest and encourages that further seismic research be carried out using LASA, not only to improve the system performance itself, but also to obtain a more detailed understanding of the earth's interior.

Section 2

PLANS

The following tasks are planned for execution during the remainder of the program. The tasks are discussed in approximate order of priority. Note that the ordering will be dependent upon the results of related tasks and the availability of time and data.

2.1 TIME DELAY STUDY

A revised linear-quadratic wavefront program will be used to process a few seismic events which have been received at LASA and whose arrival times at each subarray have been measured. An attempt will be made to organize these arrivals on a world-wide basis, and to investigate ways to make the steering delay errors reasonably small.

A modest program of measuring arrival times from LASA event tapes will be undertaken. For strong events, it is expected that one of several possible methods of thresholding will be acceptable. For weak events, the question exists whether beam gain peaking or correlation methods might provide usable arrival time differences. Hopefully, a peaking program can be written which answers this question. The objective is to develop methods of automatic arrival time difference measurement to determine the residual steering error as a function of measurement technique and array aperture.

2.2 LOGIC, EQUATIONS AND PROGRAMS FOR EVENT PROCESSING

A logic will be developed to sort and identify the manifold arrivals or detections which are expected to be made by the detection processing function. These are expected to include both side-lobe detections and subsequent phases. The routine event processing function will include this logic as well as appropriate preformed event beams and associated event location methods.

In addition, equations will be formulated and programs written for special processing of interesting events. These programs are likely to include adaptive beamformation to obtain the best possible steering delays for selected events.

2.3 DISPLAYS

A breadboard model beam display has been constructed and is ready for experimental use on taped events. Typical experiments which can now be pursued include: display of subarray "glitches" as differentiated from real events, display of the simulated system impulse response, effect on display of various combinations of time-delay errors, effect of various display intensity scales, display of detection as well as event beam patterns, operating considerations such as retention of detected arrivals until they are turned off, evaluation of various slow-motion time scales and detection techniques.

2.4 DATA ANALYSIS ACTIVITY

Results of subarray data analysis performed on the Longshot event are reported in Appendix B. This analysis, as well as LASA beam analysis and corresponding filtering and its effect on both detection and event processing performance, and other seismic events analysis, will be continued.

2.5 MICROCODE SIMULATION

Simulation of the algorithms as defined in Appendix C, with a view to attaining maximum speed efficiency in microprogramming and simulation of possible implementation techniques, will be accomplished.

2.6 DETECTION/EVENT PROCESSING CONTROL

The control function philosophy for a duplex signal processing system will be defined.

2.7 RAY TRACING

The ray tracing program may be modified to efficiently calculate post-P arrival travel times, to automatically calculate wave-front curvatures and intensity for comparison with measured curvatures, and to accept velocity profiles with a continuous velocity gradient so as to eliminate any spurious caustics.

2.8 BEAM PATTERNS

A beam pattern program to plot amplitude and phase contours will be investigated for possible application to Montana LASA beam pattern improvement and regular polygon array synthesis.

2.9 LOCATION CAPABILITY

The cross-covariance program can be applied to arrivals at world-wide seismic stations to test the capability of providing more accurate relative arrival times for improving the location accuracy capability of a potential world network, provided available records exhibit sufficient timing accuracy to support the experiment.

Appendix A

BEAM ANALYSES

A.1 INTRODUCTION

In this Appendix the activity pertinent to beam analysis is presented. The program described in Section A.2 has been employed to provide the velocity space mapping, and its description is included herein for the sake of completeness. The analysis summary in Section A.3 describes the method of estimating beam-count requirements. The dimensions of the beams are discussed in Section A.4, which together with Section A.5, constitutes a baseline estimate for event location before further beam processing. Some brief remarks concerning the generation of beam steering delays and their significance with respect to array gain are presented in Section A.5. Section A.6 contains the description of a technique which allows a reduction in subarray beamforming requirements simply by selective steering and Section A.7 concisely addresses location estimates.

A.2 VELOCITY SPACE MAPPING

The program used for preparing inverse velocity space maps of the world land areas and seismic zones, as well as lines of constant latitude or longitude, is documented in this section. The program will run in either of two modes. In Mode 1, input pairs of latitude and longitude are accepted and mapped into inverse velocity coordinates. In Mode 2, points at regular intervals of latitude and longitude are mapped to obtain coordinate lines. World map latitude and longitude coordinates used for preparing the inverse velocity map were supplied in magnetic tape format through the courtesy of the U. S. Navy Oceanographic Office and are gratefully acknowledged.

The transformation to be made consists of calculating the range and azimuth by means of spherical trigonometry and then converting range to horizontal phase velocity. The latter transformation is based on the ray tracing presented in IBM's LASA Signal Processing Study.* The present program's intended applications are to estimate beam counts, to roughly predict the relationship between geographic locations and inverse phase velocity (W), and to prepare W-space maps. It does not contain a provision to correct for the earth's ellipticity.

The quadratic formula used in this program to relate range to velocity is a close approximation to the values of $W = V_h^{-1}$ versus XDR derived in the LASA Final Report.*

The spherical trigonometry of the transformation is shown in Figure A-1. The range angle R is equal to side c of the spherical triangle ABC, and can, therefore, be evaluated from

$$\cos R = \sin \theta_o \sin \theta + \cos \theta_o \cos \theta \cos (\varphi - \varphi_o), \tag{1}$$

where:

$0 \leq R \leq 180^o$.

The azimuth is determined by

$$\sin AZI = \frac{\cos \theta \sin (\varphi - \varphi_o)}{\sin R}, \tag{2a}$$

$$\cos AZI = \frac{\sin \theta - \sin \theta_o \cos R}{\cos \theta_o \sin R}, \tag{2b}$$

where:

$0 \leq AZI < 360^o$. Both equations (2a and 2b) need to be considered to determine the correct quadrant of AZI.

*IBM Final Report, "LASA Signal Processing Study," Contract No. SD-296, July 15, 1965, p. B-9.

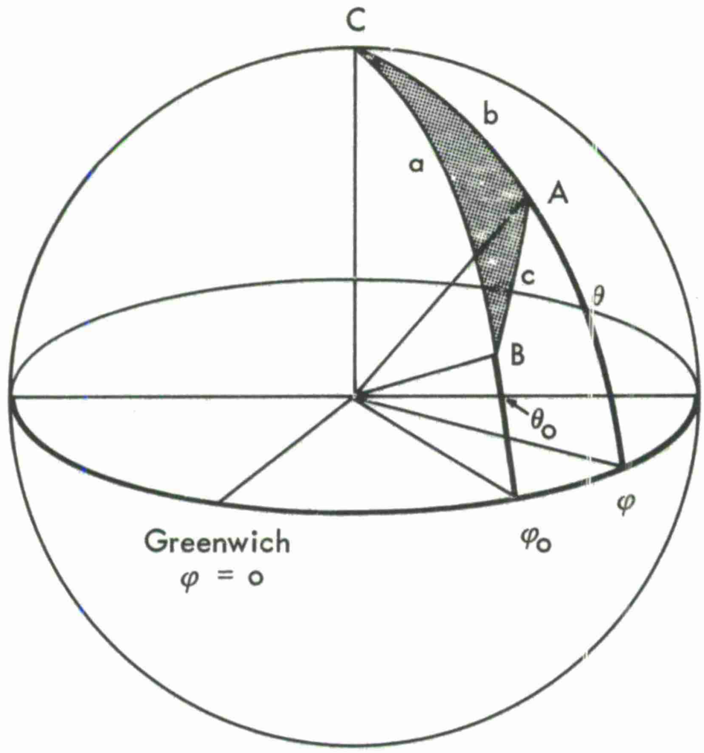

$A(\varphi, \theta)$ . . . Point at Longitude φ (East), Latitude θ (North)

(φ, θ are negative, if West or South)

$B(\varphi_o, \theta_o)$ . . . Coordinates of Receiving Array

C . . . North Pole

$R \equiv c$ = Range angle

AZI = Azimuth, angle CBA

Figure A-1. Relation of Range and Azimuth to Latitude and Longitude

From these rules, the following procedure for a computer program to calculate the $\tan^{-1}$ function with output between $-\pi$ and π is derived:

a. Range:

1. Calculate cos R from (1)

2. $\sin R = \sqrt{1 - \cos^2 R}$

3. $R' = \tan^{-1} \dfrac{\sin R}{|\cos R|}$

4. If $\cos R \geqslant 0$, $R = R'$

5. If $\cos R < 0$, $R = \pi - R'$

b. Azimuth

1. If $\varphi = \varphi_o$:

   If $\theta \geq \theta_o$, $AZI = 0$

   If $\theta < \theta_o$, $AZI = \pi$

2. If $\varphi = \varphi_o \pm \pi$

   If $\theta \geq -\theta_o$, $AZI = 0$

   If $\theta < -\theta_o$, $AZI = \pi$

3. If neither $\varphi = \varphi_o$ nor $\varphi = \varphi_o \pm \pi$, proceed as follows:

   If $\theta = \frac{\pi}{2}$, $AZI = 0$

   If $\theta = -\frac{\pi}{2}$, $AZI = \pi$

   If $\theta \neq \pm \frac{\pi}{2}$, proceed as follows:

   If $\sin\theta - \sin\theta_o \cos R = 0$, $AZI' = \frac{\pi}{2}$.

   If $\sin\theta - \sin\theta_o \cos R \neq 0$, proceed as follows:

$$AZI' = \tan^{-1} \frac{\cos\theta \cos\theta_o \sin(\varphi - \varphi_o)}{\sin\theta - \sin\theta_o \cos R}$$

If $\sin(\varphi - \varphi_o) \geq O$ and $AZI' \geq O$, $AZI = AZI'$

If $\sin(\varphi - \varphi_o) \geq O$ and $AZI' < O$, $AZI = AZI' + \pi$

If $\sin(\varphi - \varphi_o) < O$ and $AZI' \geq O$, $AZI = AZI' + \pi$

If $\sin(\varphi - \varphi_o) < O$ and $AZI' < O$, $AZI = AZI' + 2\pi$

A.2.1 Range and Inverse Horizontal Phase Velocity

The range in kilometers is the range angle R, multiplied by the radius of the earth R_E. The ray tracing to which reference has been made is closely approximated between 30^o and 95^o range by the quadratic formula

$$R_E \cdot R = A + BW + CW^2,$$

where:

$(R_E \cdot R)$ = the range in km

W = the inverse phase velocity in sec/km

A = 13,528

B = -46,116

C = -10^6.

W may thus be calculated (for $0.04 \leq W \leq 0.08$) from

$$W = -\frac{1}{2C}\left[B + \sqrt{B^2 + 4C(R_E \cdot R - A)}\right].$$

A plot of World land areas with longitude and latitude coordinate intersections is shown in Figure A-2.

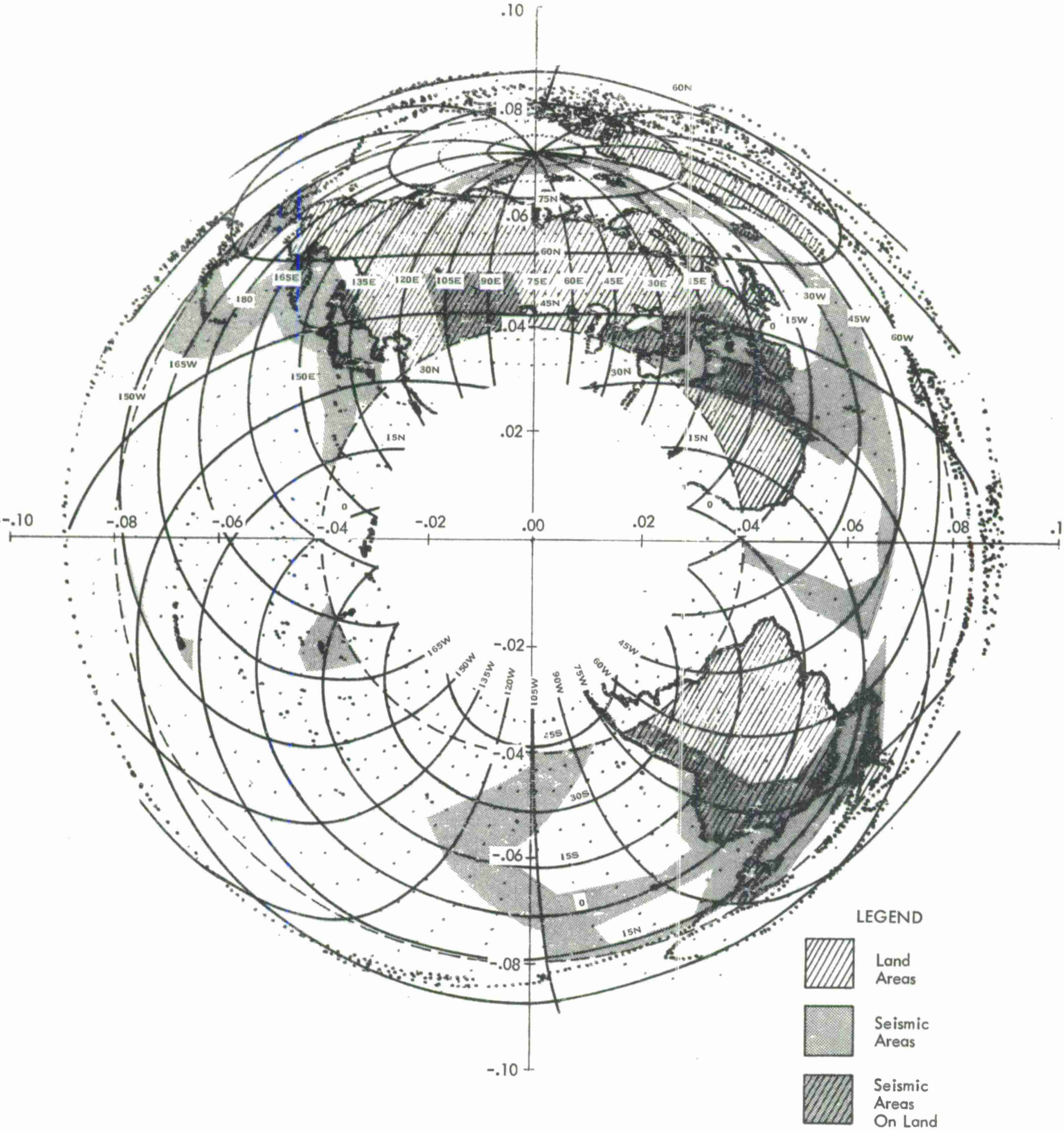

Figure A-2. Inverse Velocity Space Map of World Land Areas and Seismic Zones, Centered at Billings, Montana

A.3 BEAM REQUIREMENTS

To further check Montana LASA beam requirements for teleseismic world coverage* and to facilitate beam counts for any other possible site, a set of film templates of close-packed circles has been prepared as shown in the example of Figure A-3. These templates, when used with a W-space map such as Figure A-2, can be used to easily determine the numbers of detection beams of any size required to cover any given area for a prescribed array site. Templates with circle diameters having successive ratios of $\sqrt{2}$, and ranging from 1/16 inch up to $\sqrt{2}$ inches have been made. For circles smaller than 1/16 inch, the appropriate numbers can be estimated by dividing the map area in W-space by the area of the inscribed hexagon (for nonduplicating coverage) belonging to a single beam, since for such small beams, the edge effects on the map can be neglected.

Figure A-4 shows beam requirements for coverage of land and seismic areas, as well as land only, as a function of the W-circle diameter, as measured on a map scaled to 1 inch = 0.02 sec/km.

The value of the W diameter depends upon (1) the array used (e.g., 21 subarrays vs. 17 subarrays vs. 13 subarrays), (2) the maximum loss in db to be tolerated, and (3) the frequency at which this loss may occur.

To obtain the beam diameters in W space for practical beams, reference is made to beam patterns which have been calculated and presented in previous reports. For the main lobe, which is of concern here, the following quadratic approximations for W-space beam diameters are adequate:

21 SA LASA beams: $D = 0.0042 \sqrt{L/f}$,

17 SA LASA beams: $D = 0.0070 \sqrt{L/f}$,

13 SA LASA beams: $D = 0.0118 \sqrt{L/f}$,

9 SA LASA beams: $D = 0.0185 \sqrt{L/f}$,

Subarray beams: $D = 0.105 \sqrt{L/f}$,

where:

L = loss in db

f = frequency in Hz

D = beam diameter in sec/km.

*IBM, First Quarterly Technical Report, "LASA Signal Processing Simulation and Communications Study," Contract No. AF 19(628)-5948, May 27, 1966.

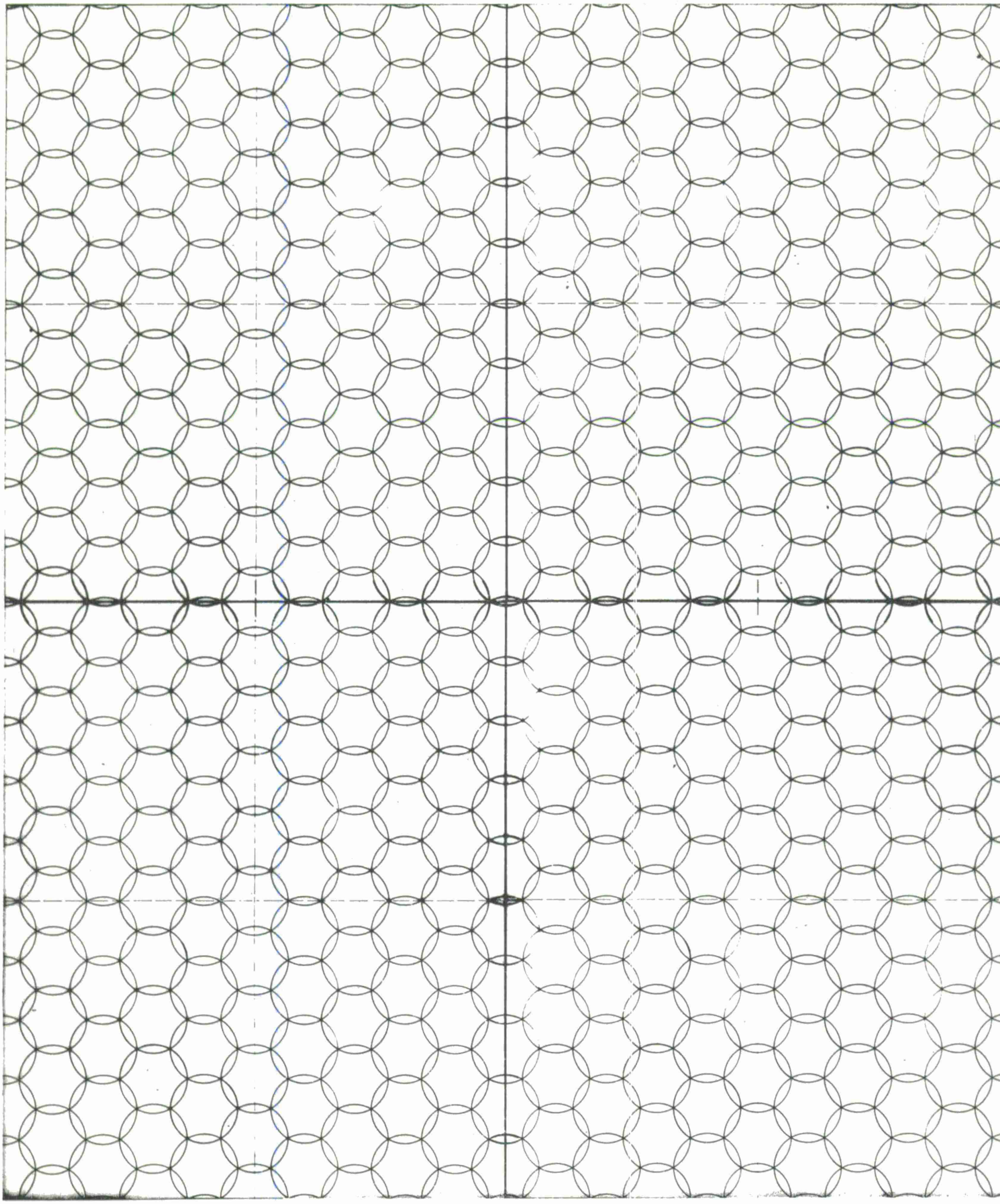

Figure A-3. Sample Template Showing Close-Packed Arrangement of Beams (Beam Diameter, D = 0.5 Inch - Corresponding to 0.01 sec/km)

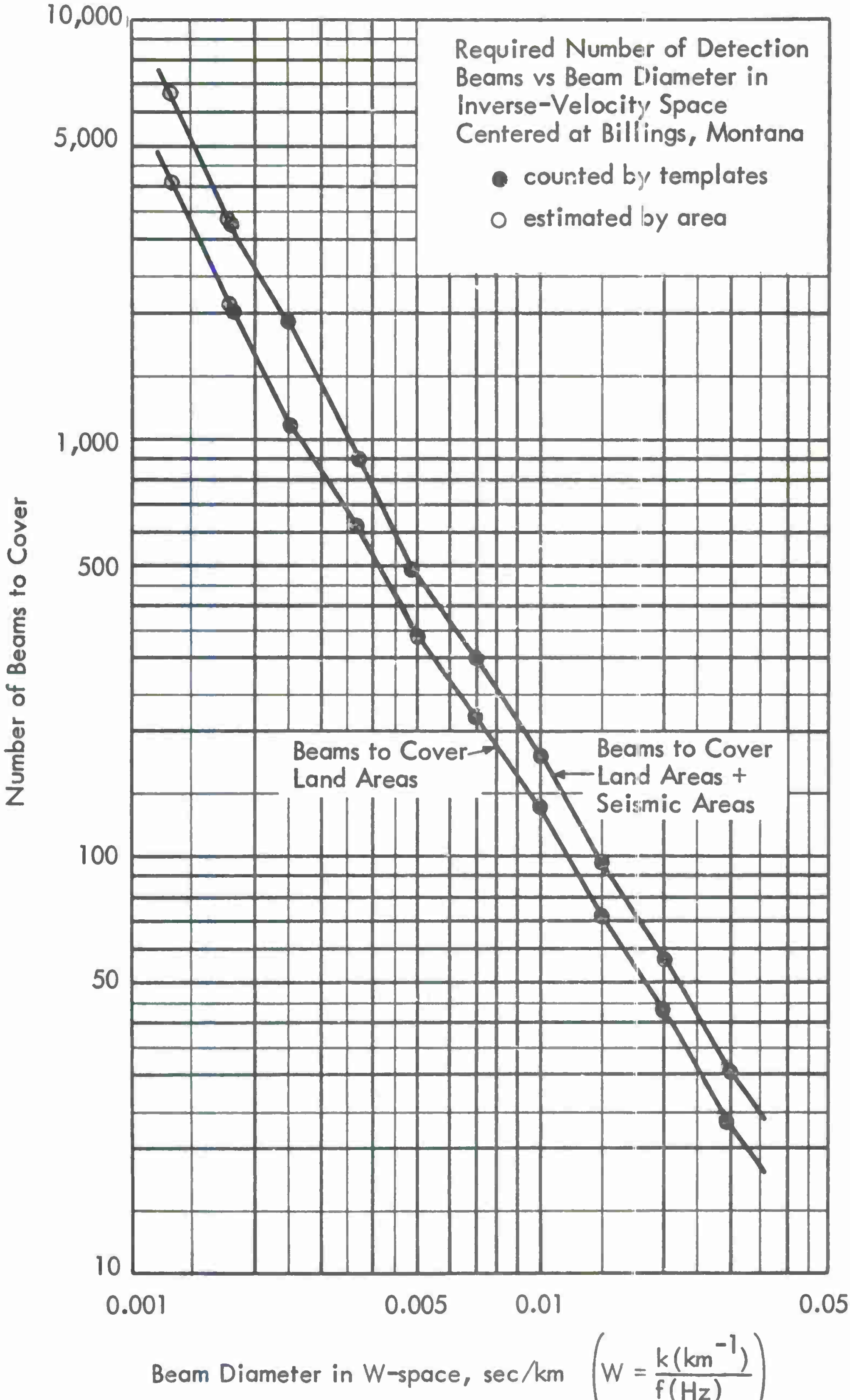

Figure A-4. Required Number of Detection Beams vs Beam Diameter in Inverse-Velocity Space Centered at Billings, Montana

As a sample calculation, let it be required to determine the number of detection beams needed to cover land and seismic areas, and permitted to lose 1.7 db (in addition to a 1.3 db subarray beam loss), at 1.5 Hz, using all 21 subarrays.

From the formula for 21 subarrays, the W-space beam diameter is $D = 0.0042 \cdot \sqrt{1.7}/1.5 = 0.0036$ sec/km. From Figure A-4, the number of such beams needed to cover land and seismic zones from Montana is N = 900. This number was previously estimated conservatively at 1000.*

A.4 BEAM DIMENSIONS

This section presents an estimate of the accuracy of event location on the earth's surface, in terms of the size of LASA beams in inverse-velocity (W) space.

The following nomenclature will be used in the tables:

W = inverse phase speed, sec/km

X_R = distance in range direction, km

X_A = distance in azimuth direction, km

$$\frac{dX_R}{dW}, \frac{dX_A}{dW} = \text{W space to geography scale factors, } \frac{\text{km}}{\text{sec/km}}$$

$$\frac{dX_R}{dW} = \frac{\Delta(XDR)}{\Delta(VH-1)} \text{ from ray trace* or}$$

$$= b + 2cW \text{ from quadratic approximation}$$

$$\frac{dX_A}{dW} = \frac{R_E \sin\theta}{W}$$

D_W = diameter of beam circle in W space, sec/km

D_K = diameter of beam circle in K (wave number) space, cycles/km

$D_K = fD_W$, where f = frequency, Hz

*IBM, First Quarterly Technical Report, "LASA Signal Processing Simulation and Communications Study," Contract No. AF 19(628)-5948, May 27, 1966, p. B-3.

R = range, km

$R = a + bW + cW^2$ is quadratic approximation to range vs. inverse phase speed relation. R in km

θ = range angle, radians (or θ^{o}, in degrees);

$\theta = R/R_E$ where R_E = radius of earth

D_R, D_A = range axis and azimuth axis of beam ellipse, km

$$D_R = \frac{dX_R}{dW} D_W; \; D_A = \frac{dX_A}{dW} D_W$$

D = larger of D_R or D_A

$a = 13{,}528$; $b = -46{,}116$; $c = -10^6$; $R_E = 6370$

Table A-1 presents the scale factors for several ranges relating small changes in inverse phase speed, W, to kilometers on the earth's surface, in the range and azimuth directions. A small single frequency constant loss circle in W-space will transform into approximately an ellipse in real coordinates. The scale factors of Table A-1 are the ratios of the range and azimuth semi-axes, respectively, to radius of the W-space circle. The scale factors of Table A-1 presented for values of W of approximately 0.04, 0.06, and 0.08, have been obtained from a previously published ray tracing.* An additional value of W = 0.0769 has been inserted because the value of $\frac{dX_R}{dW} = -409{,}800$ at W = 0.0801 is artificially high. This anomaly appears to have been caused by a "caustic" generated by a first-derivative discontinuity in the piecewise linear velocity profile used in the ray trace.

*IBM Final Report, "LASA Signal Processing Study," Contract No. SD-296, July 15, 1965.

Table A-1. Range, Range Angle, and Scale Factors Obtained From Ray Trace, Velocity Profile 2

W	R	θ	$-\frac{dX_R}{dW}$	$\frac{dX_A}{dW}$
0.0412	10454	94.0°	177,200	154,200
0.0604	6569	59.1°	131,600	90,480
0.0769	4178	37.6°	191,300	50,510
0.0801	3419	30.8°	409,800	40,660

In Table A-2, the same quantities are presented after a quadratic fit has been made to the Range versus W relationship. The artificial discontinuity near W = 0.08 has thus been removed.

Table A-2. Range, Range Angle, and Scale Factors From Quadratic Approximation to Ray Trace, Velocity Profile 2

W	R	θ	$-\frac{dX_R}{dW}$	$\frac{dX_A}{dW}$
0.04	10083	90.69°	126,100	159,200
0.06	7161	64.41°	131,600	95,700
0.08	3439	30.93°	206,100	40,900

The actual velocity profile of the earth may have significant velocity discontinuities at larger depths, and thus caustics. However, presently available data is insufficient to come to an accurate conclusion on this question. Therefore, for the present, estimates will be based on a smooth profile, so that typical scale factors would appear to range up to about 200,000 km/(sec/km).

Table A-3 presents the length in km of the larger double-semi-axis of the beam ellipse for various types of beams and the three values of W. Three db contours of 1.5 Hz detection beams are evaluated for the full LASA array (21 SA), as well as for the truncated arrays found by eliminating the outer one or two rings of subarrays, respectively. Also given are values for 21 SA, 3 Hz, 3 db event beams and 21 SA, 1.5 Hz, 3 db event beams. Beam diameters measured in this manner are thus seen to range from about 70 to 2100 km. Detection beam location for a 17 SA beam is thus of the order of 300 to 1300 km depending on range, whereas event beam resolution is of the order of 100 to 400 km.

Table A-3. Diameters for Various Beams, Using Scale Factors From Quadratic Approximation of Table A-2

Type of Beam					D km		
SA	L (db)*	f	D_K	D_W	W = 0.04	W = 0.06	W = 0.08
21	3.0	1.5	0.0073	0.0049	780	470	200
17	3.0	1.5	0.0120	0.0080	1270	770	330
13	3.0	1.5	0.0200	0.0133	2120	1270	540
21	3.0	3.0	0.0073	0.0024	380	230	100
21	1.5	3.0	0.0052	0.0017	270	160	70

*L (db) is the loss in db at the beam circumference. It is assumed that the full loss is incurred in forming the LASA beam, i.e., the subarray beams are formed with negligible loss.

A.5 ARRAY STEERING DELAYS

The loss in array gain in db, attributable to errors in steering delays is given by

$$\text{Loss} = 10 \log_{10} e \ (2\pi f \sigma)^2,$$

where: f is the signal frequency in Hz and σ the standard deviation of steering errors in seconds, i.e.,

$$\sigma^2 = \frac{1}{N} \sum_{k=1}^{N} (\delta t_k - \delta t_{ks})^2,$$

where: δt_k = the relative arrival time at the k^{th} subarray center and
δt_{ks} = the steered delay at the k^{th} subarray center.

At a detection frequency of 1.5 Hz, a standard deviation of 0.5 sec. and 1.0 sec. in the steering delays would produce losses of 1.0 db and 3.8 db, respectively. Therefore, it is important that the delays of even the presteered detection beams be known to at least an accuracy of 0.1 sec, with a standard deviation of considerably less than this value. To get the best possible gain at event beam frequencies, it is likely that some adaptive procedure such as adjusting the arrival time at each subarray for maximum array gain (beam peaking) or for maximum correlation, will be required.

The method by which the detection beam delays will be obtained must be essentially an empirical one, based on the actual arrival times of actual wave fronts received at LASA. It is expected that a large number of strong event receptions will be analyzed by means of a Least Squares Wavefront program to determine the velocity components, curvatures, and the deviations of actual arrival times from plane or quadratic wave fronts. It is hoped that when the time deviations for each group of wave fronts are averaged and compared, the standard deviations will be sufficiently small to permit accurate steering.

The regions on the earth for which such calibration delays can be measured will generally be those from which numbers of relatively strong seismic events are received. For other regions, from which only weak events are received, an interpolation method will be required.

Programs for analyzing numbers of LASA arrivals are now being completed and the task of analysis will be initiated shortly. These programs will calculate wave-front directions, velocities, and curvatures, as well as the deviations of actual from ideal arrival times. The program assumes the existence of a set of arrival times for each subarray.

The arrival time inputs to the Least Squares Wavefront program will initially be those obtained through the courtesy of the Teledyne Seismic Data Laboratory. We intend also to obtain such times for other events by simple thresholding on strong events, and by cross-correlating weaker signals to obtain more comprehensive coverage.

The wave-front deviations which have been obtained by the above procedure will be averaged appropriately to obtain sets of presteered beams for the detection processor. The event processor is expected to have an adaptive capability to adjust the steering for a given beam so as to maximize array gain for that event.

A.6 DISPERSION OF SUBARRAY BEAMS

A.6.1 Discrete Subarray Beam Steering

In subarray beam calculations to date, it has been assumed that, to cover a given region of the earth, all 21 subarrays are aimed at the center of the region. The resulting subarray beamforming loss is then zero at the center, and 1.3 db at a distance of $\delta W = 0.04$ sec/km from the center. Each of the 21 subarrays has its own set of seismometer locations, corresponding to its rotation relative to subarray E1 or C4, each of which has a long arm pointing North. Therefore, the number of separate subarray beams to be formed is 21 N, where N is the number of subarray beams per subarray, or the number of regions or sectors

to be covered. With this method of coincident coverage, N has to be equal to six for world coverage at no more than 1.3 db loss. Thus, world coverage is achieved by using 126 separate subarray beams, aimed at six discrete locations and losing from 0 to 1.3 db.

A.6.2 Azimuth Dispersion

It is possible to smooth out this loss in the azimuth direction so that the loss will no longer be as little as zero at the center, but in return it will be no greater than 0.64 db anywhere when N = 6. The corresponding losses for N = 5 or 4 are 0.76 db and 1.12 db, respectively. This smoothing is achieved by dispersing the 21 N subarray beams in azimuth, with 21 beams uniformly distributed in each sector as shown in Figure A-5. When this is done, the maximum subarray beam-forming loss using only 5 subarray beams per subarray for world coverage is 0.5 db less than when 6 subarray beams per subarray are steered discretely.

If P is a point at range R to be covered by a set of 21 subarray beams, then the 21 subarray beams S_i nearest to P are chosen. This will include one beam for each subarray. As shown in Figure A-5, all subarray beams are centered at a range c, to be determined for optimum coverage. The angle 2φ of the sector is given by

$$2\varphi = \frac{360^{o}}{N} \tag{1}$$

where: N = the number of sectors or the number of subarray beams per subarray.

The contribution to a subarray beam amplitude of the ith subarray beam is SX_i, where S is the individual signal strength and

$$X_i = e^{-ar_i^2} \tag{2}$$

Here, a is the rate of subarray beam loss fall-off with radius in inverse velocity space. For LASA subarrays at a 1.5 Hz detection frequency, a = 93.5 (km/sec)^2. As shown in Figure A-5, r_i is given by

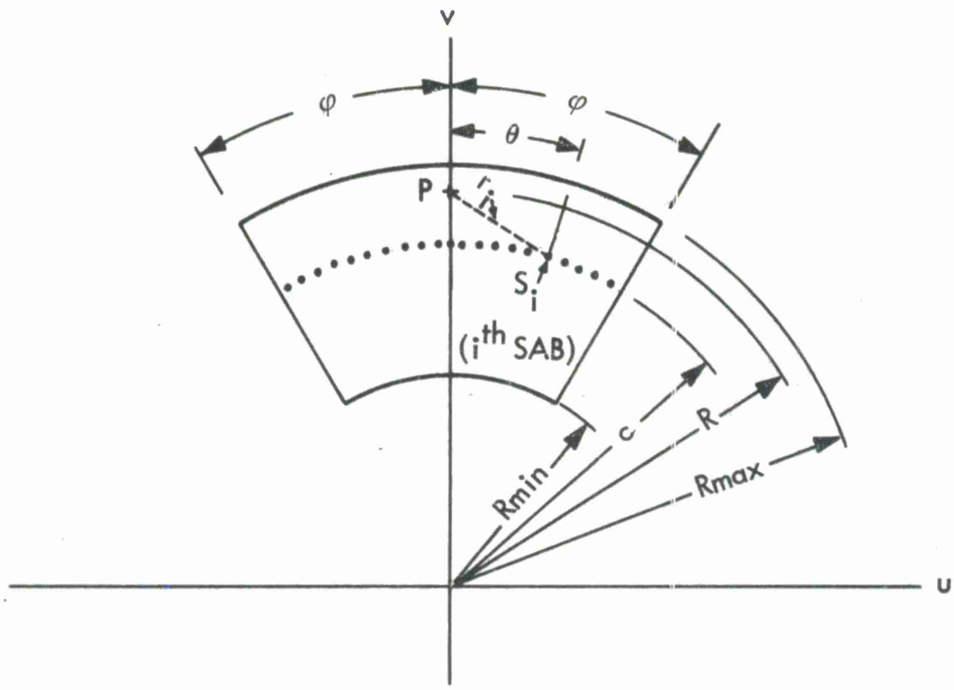

Figure A-5. Azimuth Dispersed Subarray Beam Steering in Inverse-Velocity Space

$$r_i = \left[R^2 + c^2 - 2Rc \cos\theta \right]^{1/2} \tag{3}$$

The beam amplitude is thus approximated by the integral

$$A = \frac{1}{2\varphi} \int_{-\varphi}^{\varphi} e^{-a(R^2 + c^2 - 2Rc \cos\theta)}\, d\theta. \tag{4}$$

It will be shown that for practical values of a, R, c and θ, the exponent is sufficiently small that it may be replaced by the constant and linear terms in its power series expansion. Therefore, we may write

$$\begin{aligned} A &= \frac{1}{2\varphi} \int_{-\varphi}^{\varphi} \left[1 - a\,(R^2 + c^2 - 2Rc \cos\theta) \right] d\theta \\ &= 1 - a\,(R^2 + c^2 - 2Rc \frac{\sin\varphi}{\varphi}). \end{aligned} \tag{5}$$

Moreover, the power loss resulting from subarray beam forming is thus

$$L(R) = -20 \log_{10} A. \tag{6}$$

The value of subarray beam range c will be taken such that the loss is equalized at the extreme ranges, R = 0.04 and 0.08 (sec/km), or

$$c = \frac{\varphi}{\sin\varphi} \cdot \frac{1}{2} (R_{min} + R_{max}). \tag{7}$$

The greatest loss will then occur at R = Rmin and R = Rmax, and the losses Lmax at these extreme ranges will be equal.

Table A-4 shows the value of φ (Equation 1), the best subarray beam range c (Equation 7), and worst loss Lmax (Equation 5, 6) when 6, 5, or 4 subarray beams per subarray are used in a dispersed mode to obtain world coverage; a = 93.5 $(km/sec)^2$ for 1.5 db detection subarray beams, and Rmin and Rmax are 0.04 and 0.08 sec/km, respectively. Column 5, Lmin will be discussed in Section A.6.3.

Table A-4. Numerical Values of Best Beam Range and Worst Loss for 6, 5, and 4 Subarray Beams Per Subarray

N	φ (rad.)	c (sec/km)	Lmax (db)	Lmin (db)
6	$\pi/6$	0.0628	0.64	0.28
5	$\pi/5$	0.0641	0.76	0.43
4	$\pi/4$	0.0666	1.16	0.70

It remains to show that the linear approximation to the exponential was valid. For the worst case, N = 4, a = 93.5 $(km/sec)^2$, the largest possible value of R is Rmax = 0.0575 sec/km, so that we have

$$e^{-aR^2_{max}} = 0.735, \text{ whereas}$$

$$1-aR^2_{max} = 0.691$$

This worst case shows that the linear approximation for the exponential is within about 6% and is adequate for the estimates made here.

A.6.3 Possibilities of Further Gains by Radial Distribution

To determine whether additional benefits might be obtainable by further averaging the beam losses through radial distribution of the subarray beam centers, we first look whether there is indeed anything to average, i.e., whether the minimum loss along a radius is significantly below the maximum loss at Rmin and Rmax. As shown below, a very marginal improvement might be possible.

The minimum loss occurs at a value of R such that

$$\frac{dA}{dR} = -a \ [2R - 2c \frac{\sin\varphi}{\varphi}] = 0, \text{ or}$$
$$R = c \frac{\sin\varphi}{\varphi} . \tag{8}$$

At this value of R, A has the value

$$\text{Amin} = 1 - ac^2 (1 - \frac{\sin^2\varphi}{\varphi^2}), \text{ and} \tag{9}$$

$$\text{Lmin} = -20 \log_{10} \text{Amin}. \tag{10}$$

Numerical values for Lmin are shown in the last column of Table A-4, and are in the order of 0.3 db better than Lmax. Thus, one can conclude that the addition of radial dispersion might provide a further reduction of perhaps 0.15 db in the subarray beamforming loss. In the light of our present poor knowledge of some much more important factors such as the effects of timing error, this relatively marginal improvement possibility will not be further pursued at this time.

A.7 EVENT LOCATION ESTIMATE

This section is concerned with estimating the accuracy with which a seismic event might be located by a LASA installation. Consider the cases of routine processing, and special processing for events of particular interest. An event may require special processing because its travel times and location are desired as calibration inputs to the system, or because of scientific or other interest.

In routine event processing, a bundle of event beams is centered on the appropriate detection beam center line, and used to locate the event. In this case, the following sources of location error are expected to accrue:

a. Errors due to finite beamwidth

b. Errors in beamforming due to incorrect steering delays

c. Errors in relating measured phase speed to range.

In the case of special processing, beamwidth errors (type a) will not exist and an attempt is made to minimize steering delay errors (type b). Errors relating phase speed to range (type c) will exist for both routine and special processing; their magnitude depends entirely upon the accuracy to which the source location has been previously calibrated.

The error due to finite beamwidth (a) is closely related to the beam resolution discussed in Section A.4. There, estimates of beam sizes in geographic coordinates were obtained. It was shown that event beams formed from 21 subarrays and losing no more than 3 db at 3 Hz have a range semi-axis of between 50 and 190 km. Thus, one can expect, with routine processing, to locate an event with a resolution of at least this order, provided only that the correct beam can be selected from among a bundle of event beams. Because the main part of the seismic energy is contained in a frequency band considerably below 3 Hz, and therefore, a number of beams surrounding the best one will generally "light up," two methods of selecting the correct inverse velocity space components suggest themselves.

The first is to select the inverse velocities at the center of gravity of the bundle of event beams. This method is computationally simple and has the advantage of retaining the low-frequency beam energy while at the same time permitting examination of the side-lobe structure. Another possible method might be to reduce the spread of the event beam bundle by high-pass filtering of the energized beams. The disadvantage of this would seem to be that most of the beam energy which is at lower frequencies would be disregarded.

We next turn our attention to type b errors; the effect of incorrect steering delays leading to an incorrect value of the inverse phase velocity components. As a first estimate of this error, we consider just two seismometers, separated by an array aperture of 200 km, with an arrival time error of 0.1 sec committed at one of them for a broadside wave front. At an inverse phase speed of 0.04 sec/km, the error expressed in distance would be $0.1/0.04 = 2.5$ km, or an angle of $2.5/200 = 0.0125$ radians in azimuth. At 90° range, a timing error of 0.1 sec would thus correspond to a distance of approximately 80 km.

We now estimate this type b location error due to incorrect steering delays, when using a LASA array rather than the hypothetical two seismometers. Assume N subarrays (N = 21), distributed with rotational symmetry and with distribution density decreasing linearly with distance from the center, out to a radius R (R = 100 km). We further assume statistically independent arrival time errors with standard deviation σ seconds. Then, the RMS distance between an observed versus the real source location in $W_x - W_y$ (inverse velocity) space is given by

$$\Delta W = \frac{2}{R}\frac{\sqrt{3}\,\sigma}{\sqrt{N}} = 0.00756\,\sigma \ \text{sec/km.}$$

The actual error in geographic space is given by

$$\Delta X = \Delta W \frac{dX}{dW}$$

where the derivatives are those given in Table A-2, Appendix A. The value of the derivative is shown there to vary in absolute value from 40,900 km^2/sec. to 206,700 km^2/sec, depending on range and depending on whether the range or azimuth directional derivative is considered. Thus, the distance error varies as: $\Delta X = \alpha\sigma$ km, where the values of α in km/sec are given as a function of W for the range and azimuth directions in Table A-5.

Table A-5. Location Error Parameter Values

W (sec/km)	α(km/sec)	
	Range Direction	Azimuth Direction
0.04	954	1210
0.06	1000	724
0.08	1560	310

If we were to assume an absolutely accurate knowledge of the arrival times, and consider only the effect of the quantized sampling interval of 0.05 second, the value of σ would be $1/(40\sqrt{3})$ seconds, corresponding to ΔX between 4.5 and 27 km. This error cannot be reduced by any processing scheme save a shorter sampling interval. Assuming arrival time error standard deviations of $\sigma = 0.05$ sec. (optimistic) and $\sigma = 0.1$ sec. (pessimistic), the corresponding error from Table A-5 would thus be between 15 km and 78 km, and between 31 and 156 km, respectively. These are the location errors which might reasonably be expected in special processing. They are, as expected, less than the errors incurred from routine processing by preformed event beams.

The above discussion of location accuracy for a single LASA is now briefly summarized in the light of alternative ways to process events. When preformed event beams are used to locate events, the basic timing error is that of the preformed beams compared to the actual wave front arriving, and the resulting error in W-space is numerically about that of a 3 Hz 3 db beam radius, or perhaps 50 to 190 km. In this case, subsequent beam processing such as calculating centers of gravity of beam clusters should help materially to reduce this source of error. When on the other hand, an event is treated individually with emphasis on steering a beam designed adaptively for the event, then the corresponding least squares W-space location can probably not be still further improved. This error is a minimum of 30 km due only to sampling error, but is more likely to be 50 km to 100 km for actual events. To both methods of processing must be added the additional error of W to geography conversion, which can be minimized only for areas where calibration events have been available.

Appendix B

SIGNAL PROCESSING

B.1 INTRODUCTION

In this Appendix, scaling requirements for the LASA beamformer are discussed.

In Section B.2, the arithmetic characteristics of the beamformer relevant to the topic of scaling are described.

In Section B.3, experimental results based on an analysis of Longshot data are discussed. These results, obtained by applying various bandpass filters to subarray beam outputs, can be formulated as follows:

a. Omission of the B-ring in each subarray will enhance the conventional processing by about 1 db.

b. A LASA processing gain of about 30 db, relative to an unprocessed seismometer output, can be anticipated for signals with dominant frequency between 0.8 Hz and 1.6 Hz.

c. The seismic noise level in a LASA beam can be as low as 0.03 nm.

In Section B.4, two criteria for scaling are defined. The first criterion demands the saturation level for the LASA beamformer to be $\geq$ 50 nm. This ensures that all saturating signals can be analyzed with ample signal-to-noise ratio by means of the "padded" seismometers. The second criterion requires that the round-off errors (bias as well as random) and the sampling in the LASA beamformer will degrade the performance by an acceptable amount (e.g., 1 db or less). In applying the second criterion, allowance must be made for the possibility of a seismic noise level in a LASA beam as low as 0.03 nm.

In Section B.5, scaling and sampling for two beamformer configurations are examined. To satisfy the first criterion, a total accumulated right-shift of 5 bits must be performed on the seismometer outputs prior to the formation of LASA

beams. Of this amount, it is desirable (and possibly necessary) to apply a 1-bit right-shift prior to the formation of subarray beams. However, the latter shift should be kept as small as possible to minimize the degrading effects of the round-off errors on the LASA beam outputs.

Two configurations are considered. In one configuration, bandpass filtering is applied to the subarray beam outputs but the LASA beams are not filtered. By compensating for the (predictable) bias in the LASA beams generated by the round-off errors in the beamformer, the performance loss can be held to 0.15 db (it is 0.45 db when the bias is not compensated). The second configuration applies low-pass filtering to the subarray beams and bandpass filtering to the LASA beams. Here the performance loss due to round-off errors is negligible and compensation for round-off bias is unnecessary.

Both configurations utilize a rate of 10 samples per second for the formation and filtering of subarray beams and a rate of five samples per second for the formation and filtering of LASA beams. However, the subarray beam phasing and the LASA beam phasing are implemented with resolutions corresponding to 20 and 10 samples per second, respectively (thus limiting the phasing loss to less than 0.35 db for signal frequencies up to 1.6 Hz). As a consequence, the post detection sampling rate is also five samples per second. The effect of this sampling rate on the beamformer performance can be reliably determined only by experimental means, because it not only depends on the length of the post-detection integration interval, but also on the detailed characteristics of the signal waveform. Nonetheless, a rough estimate can be obtained by assuming the signal to be a pure sinusoid. For post-detection integration of a few seconds, the loss in performance compared to analog processing will be less than 0.5 db even in "worst-case" situations for signal frequencies up to 1.6 Hz.

It is emphasized that the beamformer configurations discussed herein are intended primarily as typical examples. They by no means represent final choices.

B.2 CONFIGURATION AND ARITHMETIC CHARACTERISTICS OF THE LASA BEAMFORMER

Figure B-1 provides a block diagram for the beamforming process. It refers to the event processor as well as the detection processor.

Step 1 is outside the beamformer inasmuch as it represents the process whereby the ground motion is sensed by the seismometer and is converted to a digital output (word length: 13 bits plus sign; value of the least significant bit: 0.028 nm).

The beamforming performed in steps 2 and 4 is of the conventional (delay-and-sum) type. The sampling rate for the detection processor is 10 samples per second up to and including step 3. It is proposed to drop the sampling rate to five samples per second thereafter, provided that the LASA beam phasing be implemented with a resolution corresponding to 10 samples per second. As pointed out in Section B.5, the penalty for halving the sampling rate after step 3 is acceptable (on the order of 0.5 db or less).

For each step in Figure B-1, the output is produced in digital form. Hence, it will possess a quantum level, Q, and a saturation level, SL. Here Q is defined as the physical value of the least significant bit in the output, while SL is the output level above which overflow may have occurred in the arithmetic operations performed in the step. Both Q and SL are measured in nanometers (nm) and are always referred to the seismometer scaling as a standard. For the step 1 output: Q = 0.028 nanometers and SL = $(2^{13}-1)$ Q = 229 nm. As another example, consider step 2, the subarray beamforming. In this process, a number of seismometer outputs (e.g., K) are added to form the step 2 output. No division by K is actually performed. Yet, we shall look upon this step 2 output as the average of the K seismometer outputs. As a consequence, the quantum level for the step 2 output is Q/K, where Q denotes the step 1 output quantum level. Because the beamformer word length of 15 bits plus sign is being considered, the step 2 saturation level, SL, cannot exceed $(2^{15}-1)$ Q/K. In fact, equality holds here because the beamformer arithmetic can be designed to keep account of all overflow conditions occurring during the addition process and to compensate for it in the final result. Thus, effective overflow only occurs when the final result exceeds the register length.

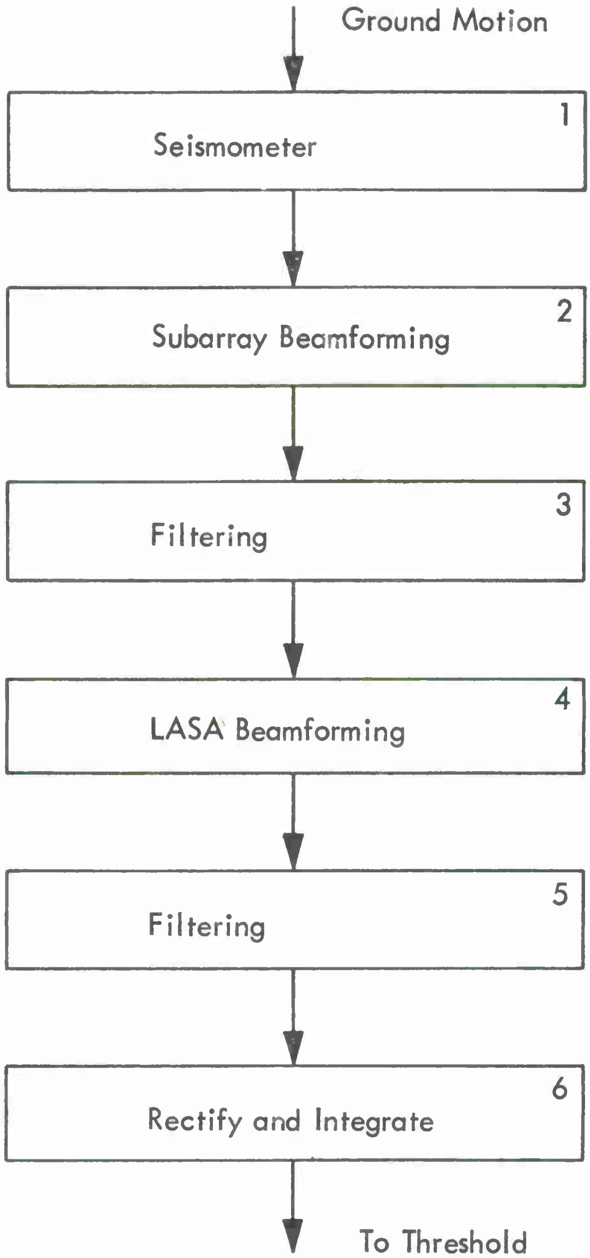

Figure B-1. Beamformer Block Diagram

We emphasize, that in this example, the absence of shift operations in step 2 has been assumed. Because Q = 0.028 nm, note that for K = 19, the step 2 quantum level and saturation level are 0.00137 and 48.3 nm, respectively.

As noted previously, the single precision word length in the beamformer is 15 bits plus sign. When "chopping" a double precision word or a right-shifted single precision word, a biased round-off error is incurred. This is a consequence of the "two's complement" arithmetic used. The bias is always negative and has its magnitude equal to half of the least significant bit. The random part of the round-off error is taken to be uniformly distributed between plus and minus half of the least significant bit. Thus, a single precision word with quantum level Q, when shifted to the right by X bits, will possess a quantum level of $2^X Q$, a bias of $-2^{X-1}Q$ and a random error with the standard deviation $2^{X-1}Q/\sqrt{3}$.

The effect of round-off can be most serious for recursive filtering, because these operations can enormously amplify the round-off errors generated in the filtering process. For this reason, in each sampling period, all products of numbers for either recursive or convolution filtering are summed using their full double precision word length and only the final result is chopped to single precision. As a consequence, at each sampling instant, only one round-off error is generated by the filtering operation.

Denoting the quantum level of the input to a recursive filter by Q, the filter output will have a bias of the form BQ/2 and a standard deviation of the form $Q\sqrt{D/12}$. For a filter of fixed degree, the values of B and D tend to increase rapidly with the sampling rate f_s (the degree of a recursive filter is the degree of the rational function in Z^{-1} describing the filter). Table B-1 lists the values of B and D for a Butterworth filter of degree six and with a pass band from 0.7 Hz to 1.4 Hz. Note that the amplification of the internally generated round-off errors for a bandpass filter can sometimes be substantially suppressed by implementing the filter as a low-pass filter running at a high sampling rate, followed by a high-pass filter running at a low sampling rate.

Table B-1. Filter Amplification Factors

f_s(Hz)	A	B	C	D
5	0	0.8	0.28	5
10	0	28.0	0.14	2,020
20	0	1394.0	0.07	2,300,000

A recursive filter also propagates and amplifies bias and random error already present in the filter input. The corresponding amplification factors will be labeled A and C (see Table B-1). If m and σ denote input bias and standard deviation of the input random error, then Am and $\sqrt{C}\,\sigma$ are the corresponding quantities for the propagated error in the filter output. In Table B-1, C has been calculated on the assumption that the random input errors are uncorrelated from one sampling instant to another. When this condition is not satisfied, an upperbound for C is furnished by the maximum value of $|H(f)|^2$, where H(f) denotes the complex (amplitude-phase) frequency response of the filter. For the filters to be considered for steps 3 and 5 in Figure B-1, this maximum value is unity, hence, $C \leq 1$.

B.3 EXPERIMENTAL RESULTS

To obtain some insight into the effectiveness of filtering as a means for increasing the signal-to-noise ratio of LASA beam outputs, a short computational analysis has been made of some of the Longshot data. The computations were performed in floating-point arithmetic using an IBM 7094.

The 25 recorded seismometer outputs of subarray B1 were delayed and summed. The sum was divided by 25 to obtain the "complete" subarray beam output. In addition, the 19 seismometer outputs, remaining after omitting the six seismometers in the B-ring of subarray B1, were likewise delayed and added. Their sum was divided by 19 to provide a "partial" subarray beam. The phasing of the seismometer traces prior to their addition was implemented with a resolution corresponding to 20 samples per second. However, both beam outputs were calculated corresponding to a real-time rate of 10 samples per second.

The complete beam, the partial beam and the output of the center seismometer, A_0, of subarray B1 were passed through the same digital recursive filter. The three outputs so obtained were used to calculate signal-to-noise ratios in the following manner. The noise power, N, was calculated by averaging the squares of 850 successive samples preceding the signal onset for each of the three channels. Thus, N is the average noise power over an 85-second time period immediately preceding the signal. The average signal power, S, for each of the three channels was calculated over an interval of 2.6 sec. This interval was chosen to yield maximum average signal power, S. The signal-to-noise ratio of each channel was defined as $10 \log_{10} (S/N)$. Note that this definition ignores the post-detection integration gain.

The filter gain for the A_0 seismometer was defined relative to the unfiltered A_0 seismometer trace. The array gain for a filtered "complete" beam or "partial" beam was computed relative to the A_0 trace after passing it through the same filter as that used for the beam. The total gain was taken as the sum of filter and array gains. The seismic noise standard deviation was defined as $\sqrt{N}$.

The results of these calculations can be found in Table B-2 for a number of bandpass filters. The filters are listed by their 3-db pass band, preceded by the designation "Bu" (for Butterworth) or "Ch" (for Chebychev). All filters were of degree six. The Chebychev filters were implemented with a 0.5-db ripple.

Note that the "partial" beam outperforms the "complete" beam by about 1 db, except for the Chebychev filter with pass band from 0.9 Hz to 3.0 Hz. The explanation lies in the fact that the low-frequency microseismic noise is strongly correlated among the seven seismometers located at the center and on the B-ring of subarray B1. Hence, the array gain for the complete beam tends to be inferior to that of the partial beam for those filters which pass more low-frequency than high-frequency noise. Thus, it is recommended that the subarray beams be formed from all subarray seismometers except those in the B-ring. This procedure will result both in enhanced signal-to-noise ratio, as well as in a lighter computational load.

Table B-2. Experimental "Longshot" Subarray B1 Data

Filter Type and Pass Band (Hz)	Noise Standard Deviation (nm)			Filter Gain (db) for A0	Array Gain (db)		Total Gain (db)	
	A0 Seismometer	Complete Beam	Partial Beam		Complete Beam	Partial Beam	Complete Beam	Partial Beam
Unfiltered	2.77	2.04	1.77	0.0	2.0	2.9	2.0	2.9
Bu 0.6-2.0	0.89	0.42	0.38	9.3	5.9	6.6	15.2	15.9
Ch 0.9-3.0	0.67	0.26	0.27	11.4	7.5	7.1	18.9	18.5
Bu 0.7-1.4	0.73	0.29	0.24	10.7	7.4	8.6	18.1	19.3
Bu 0.8-1.6	0.64	0.24	0.21	12.1	7.9	8.9	20.0	21.0
Bu 0.8-1.4	0.61	0.22	0.19	12.4	8.0	9.2	20.4	21.6
Bu 0.9-1.6	0.51	0.19	0.17	13.9	8.0	8.7	21.9	22.6
Bu 0.9-1.4	0.46	0.17	0.15	14.6	7.9	9.1	22.5	23.7
Ch 0.9-1.4	0.44	0.17	0.14	14.7	7.9	9.2	22.6	23.9

As is to be expected, Table B-2 demonstrates that the signal-to-noise ratio tends to increase as the filter bandwidth is made narrower. However, it must be remembered that different signals will possess different bandwidths. Thus, as the filter bandwidth is decreased to match the signal bandwidth, the possibility exists that the number of filters per LASA beam required to accommodate the received signals may have to be increased above unity. Hence, a compromise must be struck between the signal-to-noise ratio to be achieved and the total number of filters to be implemented. For that purpose, a preliminary analysis was made of data supplied by SDL* and listing location, magnitude and dominant signal frequency for more than 100 events received by the Montana LASA. All dominant frequencies were within the band from 0.6 Hz to 2.0 Hz. More than 85 percent were in the band from 0.8 Hz to 1.6 Hz.

According to Table B-3, the Butterworth filter with a bandwidth from 0.8 Hz to 1.6 Hz outperforms the Butterworth filter with a bandwidth from 0.6 Hz to 2.0 Hz by about 5 db. It is, therefore, tempting to conjecture that the bandwidth from 0.8 Hz to 1.6 Hz will, in fact, be adequate for the detection processor. For example, one may speculate that decreasing the lower corner frequency may not be necessary for two reasons: (1) there is a tendency for events with low dominant frequency to be also strong events; (2) because the microseismic noise level increases rapidly below 0.8 Hz, decreasing the lower corner frequency may be ineffective as a means of increasing the LASA beam signal-to-noise ratio for events with low dominant frequencies. At any rate, to decide these issues, a computational analysis, similar to that reported for Longshot, should be applied to recorded events with low dominant frequencies as well as to events with high dominant frequencies.

Pending such an analysis, the possibility must be faced that the use of a single bandpass filter will provide inadequate signal-to-noise ratio for LASA beam outputs. For this reason, two specific configurations are described and analyzed in Section B.5 for the purpose of determining a suitable scaling and assessing the loss in performance due to round-off errors.

The first configuration applies filtering to subarray beams only. The LASA beams are not filtered, i.e., the step 5 filtering (see Figure B-1) is omitted.

---

*Seismic Data Lab (Teledyne Industries, Inc.)

The step 3 filter, running at 10 samples per second, must reject both high-frequency and low-frequency noise. Thus, a bandpass filter would seem to be a suitable choice.

In the second configuration, filtering is applied to subarray beams (step 3) as well as to LASA beams (step 5); the latter filtering running at five samples per second. For example, the step 3 filtering could be (but need not be) of the low-pass type, designed to prevent "frequency folding" of the seismic noise when the sampling rate is subsequently dropped to five samples per second. The step 5 filtering could be of the bandpass type, allowing LASA beams to be filtered according to their individual needs (if required, using more than one filter per LASA beam).

The computational analysis of Longshot, reported on above, has been incomplete in the sense that the LASA beam output signal-to-noise ratio has not been experimentally determined. Experimental results obtained by the Lincoln Laboratories of MIT indicate that the additional array gain resulting from the noise suppression only, can be calculated on the conventional assumption of statistical independence of the noise at different subarrays, thus providing an added array gain of $10 \log_{10} M$ db over and above the array gain of subarray beams. Here, M is the number of subarrays used for the LASA beamforming. From this must be subtracted the signal loss due to incoherence (probably on the order of 1 db), as well as the more severe signal loss due to the usage of incorrect steering delays. This second kind of loss can occur for LASA beams steered to regions of low seismic activity. It tends to be proportional to the square of the dominant frequency and could conceivably run as high as 2 db or more. Allowing a total of 3 db for these signal losses and taking $M = 17$, it follows that the total gain for a LASA beam can be as high as $21 + (10 \log_{10} 17) - 3 = 30$ db. (Here, 21 db is assumed to be delivered by the subarray gain. See Table B-2.)

As pointed out earlier, the post-detection integration gain has been ignored in the preceding considerations. For the computational analysis of Longshot, reported on above, a post-detection interval of 2.6 seconds was used to compute the maximum average signal power, S. This somewhat arbitrary choice of post-detection integration time can be improved upon by noting that, for maximum

signal-to-noise ratio, the post-detection integration time, T, should be selected to maximize the expression $\sqrt{T}\ S$ (this assertion assumes the seismic noise to be a stationary process with a correlation time which is small compared with T). It is probably worthwhile to plot $\sqrt{T}\ S$ versus T for a number of recorded seismic events for the purpose of selecting a value of T suitable for all seismic events, i.e., entailing an acceptable loss in signal-to-noise ratio for the majority of signals. In the situation where such a compromise value cannot be established, it may be necessary to use several post-detection integration times in the detection processor.

B.4 SCALING CRITERIA

It is the purpose of this section to examine the scaling for the beamforming process as it has been defined in Section B.2. Such a scaling must satisfy the following criteria.

a. Criterion (1)—The saturation level of the beamforming process should be high enough to allow adequate detection, localization and processing of the saturating signals by means of the "padded" seismometers only (one such seismometer per subarray).

b. Criterion (2)—The round-off errors generated by the beamforming process, as well as the sampling rates employed, should degrade the LASA beam output signal-to-noise ratio by only a fraction of one db.

To satisfy criterion (1) we shall require a saturation level for the beamformer of about 50 nm or more. Because the unfiltered noise level at the LASA site is about 10 nm or less, the signal-to-noise ratio of an unfiltered saturating event, as measured by a "padded" seismometer, will be on the order of 14 db or more. This can be increased to a signal-to-noise ratio of more than 20 db by filtering using a wide pass band (e.g., from 0.6 Hz to 2.0 Hz, see Table B-2). Such a signal-to-noise ratio permits detection of saturating signals on a single "padded" seismometer and affords the feasibility of accurate timing for event localization. Hence, a saturation level of about 50 nm or more is indeed satisfactory.

To obtain a useful quantitative formulation for criterion (2), note that the bias, m, and the random error, e(t), generated in a LASA beam as a result of round-off errors in the LASA beamformer, will cause a loss in signal-to-noise ratio of the LASA beam output. This loss is given by the following expression,

$$\text{Loss} = 5 \log_{10} \left[\frac{\int_{-\infty}^{\infty} \left(\phi_n + \phi_e\right)^2 df + 2m^2 \left(\phi_n(0) + \phi_e(0)\right)}{\int_{-\infty}^{\infty} \phi_n^2 \, df} \right] \text{db.} \quad (1)$$

Here ϕ_e and ϕ_n are the power spectra, respectively, of e(t) and of the seismic noise n(t), in the LASA beam output. The derivation of equation (1) is based on the following assumptions: the total noise, n(t) + e(t), is a Gaussian stationary process with zero mean and with a correlation time which is short compared to the duration of the post-detection interval.

From equation (1), it follows that

$$\text{Loss} \approx 4.3 \frac{\sigma_e^2}{\sigma_n^2} \left(1 + \frac{m^2}{\sigma_n^2}\right) \text{db,} \quad (2)$$

where σ_e and σ_n are the standard deviations of e(t) and n(t), respectively. The approximation (equation 2) is based on the following assumptions: (1) the spectra of n(t) and e(t) are flat over their respective effective frequency bands; (2) the frequency band for e(t) extends to zero frequency, while that of n(t) does not, i.e., $\phi_n(0) = 0$; (3) the frequency band of n(t) is included in that of e(t); (4) nonetheless, the ratio of these two frequency bands can be approximated by unity; (5) σ_e/σ_n is appreciably less than unity. These assumptions are rather drastic in view of the real situation. They tend to make the approximation (equation 2) conservative, i.e., usage of equation 2 tends to overestimate the loss caused by the round-off errors in the beamformer.

Henceforth, equation (2) will be applied when examining whether the scaling of the beamforming process indeed complies with criterion (2). For these applications, it is necessary to have an estimate for σ_n. According to Table B-3, the noise standard deviation for a subarray beam can be as low as 0.14 nm. Hence, for a LASA beam, using all 21 subarrays, the noise can be as low as $0.14/\sqrt{21} = 0.03$ nm. Henceforth, when applying equation (2), we shall assume $\sigma_n = 0.03$ nm.

B.5 SCALING CONSIDERATIONS

In this section, the scaling requirements and the effects of round-off errors are discussed for two configurations of the LASA beamformer. Referring to Figure B-1, in the first configuration, the step 3 filter is a sixth degree Butterworth filter with its 3-db pass band from 0.8 Hz to 1.6 Hz. The step 5 filter is omitted, i.e., the step 4 output and the step 5 output are identical. In the second configuration, the step 3 filter is a low-pass third degree Butterworth filter with its 3-db cut-off at 2 Hz. The step 5 filter is taken to be a sixth degree Butterworth filter with the 3-db pass band from 0.7 Hz to 1.4 Hz. The step 3 filter for both configurations is implemented to run at a rate of 10 samples per second. The step 5 filter is intended to run at 5 samples per second.

As already explained in Section B.3, the first configuration can be used if one single filter applied to all LASA beams is capable of providing adequate detection capability. In the eventuality that such is not the case, and that different LASA beams require different filters or that a LASA beam must be monitored using more than one filter, the first configuration cannot be employed and an implementation similar to the second configuration may be necessary.

We begin by discussing the requirement imposed by criterion (1) formulated in Section B.4. Disregarding for the moment the filtering performed at step 3 (see Figure B-1) and assuming that M subarrays are used to form a LASA beam, it follows that the step 4 quantum level is $2^X Q/KM$ and that its saturation level is $(2^{15}-1)\,2^X Q/KM$. Here, Q is the step 1 quantum level, i.e., Q = 0.028 nm, and K is the number of seismometers used per subarray. The integer X is the total number of bits shifted from the step 1 output up to the point where the delay-and-sum process is performed in step 4 to produce the LASA beam. A positive value of X indicates a right shift.

We assume that M is chosen between 17 and 21, and that K lies between 19 (when the B-ring is omitted, see Section B.3) and 25. Hence, the saturation level for step 4 will lie between 1.75×2^X and 2.84×2^X nm. For $X = 5$, these values are 56 and 91 nm. Criterion (1) in Section B.4 demands a saturation level of about 50 nm or more. Hence, a total accumulated right-shift of 5 bits is required to satisfy criterion (1) for the step 4 processing.

This total right-shift of 5 bits only ensures that criterion (1) is met for the step 4 processing. However, it also should be satisfied for all other steps as well. Specifically, for the step 2 output, the saturation level is $(2^{15}-1)\,2^y Q/K$ nm, where y is the number of bits of right-shift applied to the step 2 input prior to the delay-and-sum process. For K = 19, this saturation level is 49×2^y nm and for K = 25, it is 37×2^y nm. Hence, to satisfy criterion (1), no right-shift is needed for the step 2 input when K = 19, while a right-shift of one bit is adequate when K = 25. Of course, for larger right-shifts criterion (1) will still be satisfied. However, it will be shown below that minimization of the effect of round-off in the LASA beam output (i.e., in the step 5 output) demands a minimum value of y, i.e., demands a minimum right-shift of the step 2 input.

This brings us to the filtering in steps 3 and 5 (see Figure B-1). Note that the filters to be implemented for the two configurations all have a complex (amplitude-phase) frequency response whose absolute value nowhere exceeds unity. This fact, together with the sinusoidal character of the signal waveform, will cause the saturation level of the filter output to be approximately equal to that of the filter input. Hence, provided that no right shifting is performed on the step 3 and the step 5 inputs prior to the filtering, criterion (1) will be satisfied for all steps up to and including step 5, if it is fulfilled for steps 2 and 4 as discussed above. Nonetheless, to provide a margin of "safety" for the step 3 filtering, it is prudent to take y = 1 (i.e., to right-shift the step 2 input by one bit) even when K = 19. The scaling for step 6 will be discussed separately.

Next, criterion (2) of Section B.4 must be applied. Particularly, the integer y defined above must be so chosen that the effect of round-off in the final step 5 output is minimized. To check whether criterion (2) is satisfied, the loss in signal-to-noise ratio of the step 5 (i.e., the filtered LASA beam) output must be

calculated using equation (2) given in Section B.4 and taking $\sigma_n = 0.03$ nm. Thus, it is necessary to calculate the bias, m, and the standard deviation, σ_e, of the round-off errors generated in the step 5 output. This can be done by calculating, for each of the steps 2, 3, 4 and 5 in Figure B-1, the quantum level, round-off bias and round-off variance for the input and the output. The description of the beamformer arithmetic given in Section B.3 will furnish the ground rules for these calculations.

As an example, consider the step 3 filtering. Because of the right-shift of the step 2 input by y bits, the step 3 input has the following characteristics:

$$\text{quantum level} = 2^y Q/K$$

$$\text{round-off bias} = a(y)\, 2^{y-1} Q$$

$$\text{round-off variance} = a(y) \left(2^{y-1} Q\right)^2 / 3K.$$

Here, $a(y) = 0$, when $y = 0$ (to indicate absence of bias errors in the step 2 output when no right-shift is applied to the step 2 input); while $a(y) = 1$, when $y > 0$. Therefore, the step 3 output has the following characteristics:

$$\text{quantum level} = 2^y Q/K$$

$$\text{round-off bias} = \left(a(y)A + \frac{B}{K}\right)\left(2^{y-1} Q\right)$$

$$\text{round-off variance} = \left(a(y)C + \frac{D}{K}\right) \left(2^{y-1} Q\right)^2 / 3K,$$

where: A, B, C, D = the amplification factors of the step 3 filters.

These factors are defined in Section B.2. The factor C refers to the propagation of random errors which are statistically uncorrelated from one sampling period to another.

The same technique can be used for steps 4 and 5. Remember that a total right-shift of 5 bits is required prior to the step 4 sum-and-delay process. Hence, a right-shift of 5-y bits must be applied to the step 4 input. In this manner, the following expressions for the quantum level, the round-off bias, m, and the round-off variance, σ_e^2, in the step 5 output are obtained:

$$\text{quantum level} = 2^5 Q/KM \tag{3}$$

$$m = \left\{ A_1 \left(a(y)\, A + \frac{B}{K} \right) 2^{y-1} + \left(A_1 + \frac{B_1}{M} \right) \frac{2^{5-1}}{K} \right\} Q \tag{4}$$

$$\sigma_e^2 = \left\{ C_1^* \left(a(y)\, C + \frac{D}{K} \right) 2^{2(y-1)} + \left(C_1 + \frac{D_1}{M} \right) \frac{2^{2(5-1)}}{K} \right\} \frac{Q^2}{3KM} \tag{5}$$

Here, A_1, B_1, C_1, C_1^*, D_1 are the amplification factors of the step 5 filter. C_1 is the factor for the propagation of that part of the random input error which is uncorrelated from sample to sample, while C_1^* applies to the part of the random error which is correlated from sample to sample. As explained in Section B.3, for the filter considered here we have $C_1^* \leq 1$. These expressions are valid for both configurations. Note that m and σ_e^2 are minimized by choosing y as small as possible. Hence, for minimum effect of round-off error, the amount of right-shift of the step 2 input should also be minimum. Thus, one should select y = 0, when K = 19 and y = 1, when K = 25.

We shall now discuss each configurations separately. For both configurations we take K = 19, M = 21, Q = 0.028 nm, σ_n = 0.03 nm. For both configurations we shall examine the case where y = 0 as well as that where y = 1 (as pointed out earlier, y = 1 is a reasonable choice even for K = 19).

B.5.1 First Configuration

The step 3 filter is a sixth degree Butterworth filter with the pass band from 0.8 Hz to 1.6 Hz. Its amplification factors are A = 0, B = 13.7, C = 0.17 and D = 560. Because the step 5 filter is omitted, we have $A_1 = C_1 = C_1^* = 1$ and $B_1 = D_1 = 0$. Hence, by applying the equations (2), (3), (4) and (5), the results in Table B-3 are obtained. The quantum level, m and σ_e, are in nanometers (nm).

Table B-3. Performance of First Configuration

y	quantum level	m	σ_e	loss (db)
0	0.00224	0.0337	0.0037	0.145
1	0.00224	0.0438	0.0053	0.422

Although the loss is acceptable for y = 1 as well as y = 0, note that it is appreciable for y = 1. The main reason lies in the large value of the round-off bias, m, which exceeds σ_n in both cases. Fortunately, this bias is perfectly predictable. Therefore, it can be reduced to less than the quantum level by adding to every LASA beam an extra constant channel whose value is the opposite of m. By doing this, the losses for y = 0 and y = 1 are reduced to 0.065 and 0.145 db, respectively.

The system performance is rather sensitive to the step 3 filter choice. For example, take y = 1 and assume the step 3 filter to be a sixth degree Butterworth filter with a pass band from 0.7 Hz to 1.4 Hz (running at 10 samples per second). Then m = 0.065 and $\sigma_e = 0.009$ nm. The loss in performance is 2.2 db. This loss is excessive, and it is mandatory to compensate for the large but predictable value of m, using the technique just explained. In this way, the loss will be reduced to 0.4 db.

B.5.2 Second Configuration

The step 3 filter is a low-pass Butterworth filter of sixth degree, with 3-db cut-off at 2.0 Hz and running at 10 samples per second. Its amplification factors are A = 1, B = 1.3, C = 0.4 and D = 1.4. The step 5 filter is a sixth degree Butterworth filter with 3-db pass band from 0.7 Hz to 1.4 Hz and running at five samples per second. According to Table B-1, its amplification factors are $A_1 = 0$, $B_1 = 0.8$, $C_1 = 0.3$ and $D_1 = 5$. The factor $C_1^* = 1$, thus overestimating σ_e as well as the loss in step 5 output signal-to-noise ratio.

For y = 1, it is found that m = 0.0009 and $\sigma_e = 0.0022$ nm. Thus, the performance loss is 0.023 db. This loss is insignificant and will be even less for y = 0. Thus, in contrast to the first configuration, it is not necessary to compensate the LASA beam outputs for round-off when using the second configuration.

It is particularly instructive to compare the loss of 0.023 db with the loss of 2.2 db calculated above for the same bandpass filter, but running it at 10 samples per second instead of five samples per second, (see Section B.2, Table B-1).

Before turning our attention to the round-off errors in step 6 (see Figure B-1), it is pointed out that a loss in performance will occur as a result of the discrete phasing of the beamforming process in steps 2 and 4. This phasing is implemented with a time resolution corresponding to a rate of 10 samples per second. The loss in signal power is proportional to the square of the dominant signal frequency and is 0.14 db at 1 Hz and 0.58 db at 2 Hz.

The results obtained so far in this section indicate that, at the price of an acceptable loss in performance, the beamformer will produce an unsaturated waveform for signal amplitudes up to 50 nm. These waveforms can be used for accurate event magnitude determination, timing and localization and for general waveform analysis.

To complete this section, consider the rectify-integrate process (step 6 in Figure B-1). In this step, a short-term and a long-term average of the rectified LASA beam output are calculated for each LASA beam output. These two averages are compared with each other for the purpose of event detection. We shall not concern ourselves with the thresholding process but confine ourselves to the calculation of the two averages.

We begin with the short-term average. Overflow can occur when signal is present. This will not degrade the detection capability, but will affect the event magnitude, timing and localization calculations. However, these calculations can then be made using the signal waveform without post-detection averaging. As a consequence, overflow of the short-term rectified signal average does not lower the effective signal saturation level of the beamformer.

No round-off error need be incurred for the short-term average. For example, straightforward addition could be used, always subtracting the oldest rectified sample while adding the most recent rectified sample. For a rate of five samples per second and an averaging interval of 2.5 seconds this method appears quite feasible.

This brings us to the effect of the post-detection sampling rate of five samples per second. The noise standard deviation of the discrete sampled average is always larger than that of the corresponding analog average. However, the loss in performance incurred is insignificant for the LASA beams, being on the order of only 0.03 db. In addition to this loss, there is also a difference between the sampled and the analog averaged signal power. Sometimes, the sampled average is higher than the analog average, and sometimes, it is lower, depending on the location of the signal onset relative to the nearest sampling point. The term "signal power average" means the maximum signal power average obtainable for a post-detection integration interval of fixed duration but with an arbitrary beginning point for the analog case, and an arbitrary first sampling instant for the sampled case. A quantity of interest is the maximum possible loss in signal power due to sampling (measured in db). This quantity not only depends on the post-detection integration duration, T, and on the sampling interval, ΔT, but also on the signal waveform. For this reason, it can be determined reliably only by experimental means. Nonetheless, it is of some interest to obtain a rough estimate. Assuming the signal to be a sinusoid of frequency f, it can be readily shown that the maximum loss is given by:

$$\text{Maximum Loss} \approx 4.3 \left[1-2\pi f\Delta T \ \cot(2\pi f \Delta T)\right] \cdot \left|\frac{\sin 2\pi fT}{2\pi fT}\right| \text{db.}$$

For $T = 2$ sec and $\Delta T = 0.1$ sec (for a rate of 10 samples per second), the maximum loss is less than 0.1 db when f is less than 2 Hz. Thus, the sampling loss is insignificant for a rate of 10 samples per second. Next, assume $\Delta T = 0.2$ sec. Then, the maximum loss is always less than 0.2 db when f is less than 1 Hz. It is less than 0.38 db when f is less than 1.5 Hz, and less than 0.78 db when f is less than 2 Hz. Because we are dealing here with the "worst possible" situation, it would seem that the losses are certainly acceptable when f is less than 1.5 Hz (which is the case for the majority of the seismic events observed). For a signal frequency of 2 Hz, the loss can be as high as 0.78 db. However, even here it must be emphasized that this is "worst case." For 50 percent of such signals, depending on the signal onset, the loss is no more than 0.2 db.

Because the computational load is significantly reduced when forming LASA beams at five samples per second rather than 10 samples per second, it appears worthwhile to accept the performance losses associated with the rate of five samples per second (we emphasize that the LASA beam phasing must have the resolution consistent with a rate of 10 samples per second).

Next, consider the long-term average. It is primarily intended to furnish the noise background estimate relative to which the threshold operations must be performed. The long-term average will be calculated by feeding the rectified LASA beam output through an exponential integrating filter (i.e., $y(m+1) = y(m) + A\,[x(m) - y(m)]$, where y(m) denotes the long-term average while x(m) denotes the short-term average of the rectified LASA beam output). As noted before, x(m) can be accumulated without round-off error by direct summation. Scaling must be implemented in such a manner that neither overflow nor severe round-off errors occur in y(m) for integration times, t, on the order of 200 seconds (t and the filter coefficient A are related by $tAf_s = 1$ where f_s is the sampling rate for x(m)).

To determine whether these scaling requirements can be met, note that the mean value of y(m) is approximately σ_n while its standard deviation is about $\sigma_n / \sqrt{Wt}$. Here σ_n designates the standard deviation of the total (i.e., seismic plus round-off) noise in the step 5 output while W is its bandwidth. A typical value of W is one Hz. From Section B.4, 0.03 nm is a reasonable minimum value of σ_n. Thus, the minimum standard deviation for y(m) comes to 0.002 nm, taking t = 200 seconds.

The round-off error in y(m) has a bias of $Qtf_s/2$ and a standard deviation of $Q\sqrt{tf_s/24}$, where Q is the quantum level of y(m). It is reasonable to demand a scaling for which this bias is small compared to 0.03 nm, while the round-off standard deviation is small compared with 0.002 nm. Taking $f_s = 0.5$ samples per second (corresponding to short-term averaging over two seconds) and $Q = 10^{-4}$ nm, the round-off bias comes to 0.005 nm and the round-off standard deviation to 0.00014 nm, the scaling requirements are readily satisfied. Because the bias is predictable, it can be removed if desired.

The saturation level is 2^{15} Q = 3.2 nm. This level is more than adequate, i.e., it is unlikely for y(m) to exceed that level. This can be seen as follows. The

seismometer noise level is on the order of 10 nm or less. Allowing only a 20-db total LASA gain (instead of the anticipated 30 db, see Section B.3), one obtains $\sigma_n = 1$ nm. This maximum noise level still is three times below the saturation level. Thus, the scaling requirements for the long-term average of the rectified step 5 output can be readily met.

Appendix C

PROCESSING SYSTEM

C.1 INTRODUCTION

In the First Quarterly Technical Report* a functional system description was given and certain operating parameters were addressed. This Appendix extends some of those considerations, and in addition, indicates methods of implementation of some of the techniques suggested in Appendices A and B of this report.

Section C.2 discusses microcoding, presents the algorithms and addresses the precision capability. The experimental display, a breadboard constructed to assist in developing and evaluating automatic "best beam" recognition characteristics is discussed in Section C.3.

In Section C.4, the overall system is described in operational terms. The functions of the interface equipments, maintenance and operation consoles and displays are presented. This Appendix concludes with Section C.5, an examination of system operational reliability in the detection mode and indicates the improvements possible with the repairable duplex system approach.

C.2 MICROPROGRAMMING

In the First Quarterly Technical Report,* a system approach was presented for on-line seismic detection using LASA. This approach involved the use of five signal processing algorithms:

---

*IBM, First Quarterly Technical Report, "LASA Signal Procesing Simulation and Communications Study," Contract No. AF 19(628)-5948, May 27, 1966.

a. Recursive filter

b. Convolution filter

c. Beam form

d. Rectify and integrate

e. Threshold

To achieve a maximum speed advantage these algorithms can be implemented using the technique of microprogramming. This technique allows the algorithms to be used as if each were a normal machine instruction.

During this quarter, a study and definition of the algorithm specifications has been underway. One of the primary premises for this work was to maintain as much generality as possible for the application of each instruction, but to also minimize the instruction execution time. The results of the work are presented in the following sections.

C.2.1 Recursive and Convolution Filters

These two algorithms are combined because of the similarity in their solution. The two equations are:

a. Recursive Filter

$$g_{ij}(n\Delta t) = 2^{\alpha}\left\{\sum_{p=0}^{P-1} a_{pij} f_i((n-p)\Delta t) + \sum_{p=1}^{P-1} b_{pij}\, g_{ij}((n-p)\Delta t)\right\}$$

b. Convolution filter

$$g_{ij}(n\Delta t) = 2^{\beta}\left\{\sum_{m=0}^{M-1} c_{mij}\, f_i((n-m)\Delta t)\right\}$$

$$i = 1, 2, \ldots, I; \quad j = 1, 2, \ldots, J.$$

For both of the above equations, all data and coefficients will have a precision of 15 data bits. The internal summations will both be carried to a precision of 31 data bits, and the outputs can be selected as any 15 out of the 31 data bits. However, intermediate summations may extend upward to 38 data bits with no arithmetic overflow indication, provided that the final summation does not exceed 31 data bits. Filter orders as large as 127, and i and j subscripts as large as 32,767 are allowed.

The input data for both of these processes (f_i, g_{ij}) is stored in blocks called threaded lists. This means that each block of data representing one time sample is chained to the block of data for the previous time sample. By adjusting the chaining addresses, processing rate changes can be effected with a one-time software change and no change in the algorithms. This technique also allows processing to proceed in nonconsecutive sample periods using data from consecutive sample periods.

C.2.2 Beamforming

The beamforming equation is

$$B_j(n\Delta t) = 2^{\alpha} \left\{ \sum_{i=1}^{I} f_i(n\Delta t - \tau_{ij}) \right\}, \quad j = 1, 2, \ldots, J.$$

For this operation the input data will be 15 data bits with a result field of 15 data bits. However, intermediate summations may extend upward to 22 data bits with no arithmetic overflow indication, provided that the final result does not exceed 15 data bits. This algorithm can process up to 32,767 beams, forming each one from up to 32,767 inputs. The τ_{ij} delay values can have a time resolution equivalent to that of the input data, regardless of the rate at which beamforming is performed.

The beamforming algorithm will use the batched concept in which five time samples of a particular beam are formed simultaneously. This grouping reduces the computation time by about 43% because the delay value must be accessed

only once instead of five times. The value five was chosen because it represented the point at which the percentage time gain started to level off.

C.2.3 Rectify/Integrate and Threshold

These two algorithms are treated together because their function will be combined into one instruction. The equations to be solved are:

$$y_j(n\Delta t) = 2^{\alpha_j} \left\{ \sum_{S=0}^{S-1} \left| x_j((n-s)\Delta t) \right| \right\} \tag{1}$$

$$z_j(n\Delta t) = 2^{\eta j}\left[y_j(n\Delta t)\right] - 2^{\mu j}\left[z_j((n-1)\Delta t)\right] + z_j((n-1)\Delta t) \tag{2}$$

$$z_j(n\Delta t) = z_j((n-1)\Delta t) - y_j((n-N)\Delta t) + y_j(n\Delta t) \tag{3}$$

$$j = 1, 2, \ldots, J.$$

In this instruction, all input and output data will be 15 data bits. There is no provision for intermediate summation overflows.

The above three equations are used in solving for a short-term integration value to reflect the averaged signal. Equation (1) is always solved followed by either equations (2) or (3). This allows a sliding "window" look at the data, reducing the number of times the instruction must be executed. In solving a long-term integration for noise level, equations (2) or (3) are used. The inputs to these equations may be either beam values or the short-term value allowing alternate methods of computing the long-term average.

The threshold level is set by using the equation:

$$T_j = u_j * z_j(n\Delta t) \tag{4}$$

After an event has been detected, a different threshold can be set by changing the value of u_j. The z_j $(n\Delta t)$ used is the result of the long-term integration and this threshold is compared to the short-term average. When this threshold is exceeded for Q sample periods out of Q' consecutive sample periods, a detection is declared. The present long-term integration value is held until the event no longer exceeds the threshold, at which time long-term averaging is resumed. The output of the threshold section is a list of beam parameters for beams which have exceeded the threshold criterion.

C.3 EXPERIMENTAL DISPLAY

The investigation of methods of displaying event beams is currently concentrated on the pattern produced by the LASA beam intensities. Beams are formed and positioned according to their relationship in the inverse velocity plane. Suggested techniques to isolate the best beam include determining the center of gravity and/or moments of the beam intensity patterns, and pattern recognition. Evaluation of these techniques would be facilitated by a visual presentation of the beam intensity pattern as a function of time. This requires a display with intensity modulation of a matrix of points in the x-y plane. An experimental display facility for this study has been constructed. The display utilizes a magnetic tape for data input and display control and a standard oscilloscope with Z-axis input as the output. A special unit provides the interface between the magnetic tape unit and the oscilloscope. This interface unit includes the necessary digital-to-analog converters and their control logic. A block diagram of the display facility is shown in Figure C-1.

The display tape is machine generated with a compatible tape drive unit. Each display tape runs for approximately 6 minutes which may represent real time, or be time compressed or expanded, as desired. Time scaling is performed when the display tape is written.

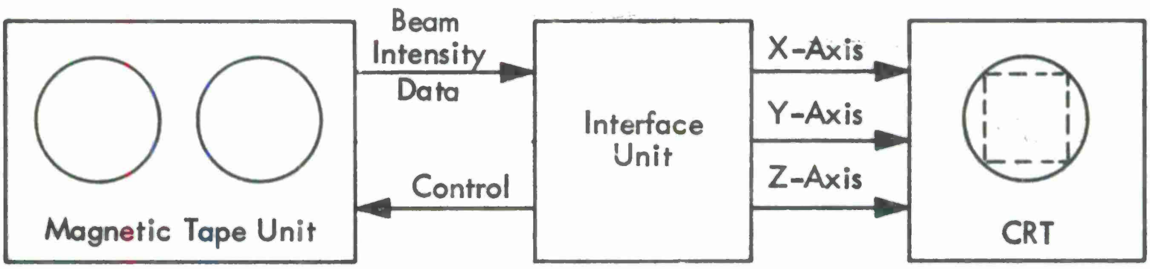

Figure C-1 Display Facility Block Diagram

The display has the capability of generating 16 levels of intensity for 1024 beams in a square matrix. Each beam appears as a square, however, its size is controllable to eliminate dark areas between adjacent beams. The patterns may be generated at rates up to 60 per second, thereby, eliminating flicker due to the pattern fading between writings.

C.4 OPERATIONAL AND MAINTENANCE CONSIDERATIONS

Within this section, the processing equipment configuration and operator functions and requirements are discussed relative to system design.

C.4.1 Data Acquisition

Raw LASA data is transmitted from each subarray equipment vault to the Data Processing Center as digitally encoded serial characters with word parity checking. This format is not compatible with general-purpose digital processing terminals, and thus, an Interface Subsystem Equipment (ISE) requirement exists to preprocess the data. Maintenance and logistics support will be most efficient if the same technology is utilized throughout the center. Such a concept dictates compatible signal specifications, thereby ensuring a minimum impact in the event of subsequent functional changes or design adjustments.

The basic function of the ISE is to buffer communication terminals, multiplex input channels, synchronize the message framing, decode the characters utilized in transmission, verify message fidelity, and translate the format to be compatible with the detection processor terminal. A secondary function is the complement processing required for a duplex communication capability to time and control each subarray. The principal design guideline should be programmed flexibility to ensure the initial interface with the dynamic subarray electronics configuration, to permit efficient subsequent upgrading of the subarray channels, and to provide latitude for the system evolution characteristic of R&D efforts. Because of anticipated LASA concept extensions, a growth potential is recommended to optimize the LASA program design efforts.

The most stable requirement item is the physical capability to interface with commercially available digital terminal equipment operating at one of the standard modular channel bandwidths. Bell half-group facilities are adequate to couple each subarray, and have been utilized in the present instrumentation.

Supporting simultaneous communications through a sufficient number of these channels constitutes a rudimentary ISE baseline requirement which can be detailed while retaining system flexibility. Buffering asynchronous input data, clocking output data, and coordinating terminal operation via the available discrete monitor and control functions are the principal interface design considerations.

Bell 303A10 Data Sets operate at a 19.2 KHz clock rate which is slow when compared with present digital technology. Early channel multiplexing is implied if the ISE hardware is to be efficiently utilized. Because this is the first unification of data, redundancy must be provided to retain the fail-soft capability afforded by the processor system architecture. The simplest method of achieving this redundancy with a minimum design expenditure is to provide dual identical channels coupled to the event and the detection processors, respectively, and to provide instrumentation to a control and coordination channel enabling smooth transitions of data flow in the event of scheduled maintenance or equipment malfunction.

Message formats are periodic with a 20 Hz rate, thereby, greatly simplifying the problem of maintaining synchronous communication. Two terminal modes evolve; the first to initially capture frame coincidence, and the second to verify proper message format interpretation while operating with a priori frame phase intelligence. Residual effects of transients are eliminated by continuously referencing all communication timing to one system standard; and because observed propagation jitter varies relatively slowly, mode throwback would be extremely rare.

Parity error control is presently employed at the word level. Message bits are encoded as characters with suboptimal entropy. These must be detected and reduced to form a binary message compatible with general-purpose digital processors. Invalid characters may be correctable if a minimum Hamming distance error is assumed and a most probable character can be recognized.

Because a discrepancy would have been detected, and character substitution is based on supposition, the word should be flagged as marginal data. Such channel creditability qualifiers may also originate from alternate indicators such as word parity, data set AGC level, or keys from the maintenance console.

The exact format translations that must transpire in the ISE are a function of the installation configuration and the detailed design of the electronics located at the subarray vault. Because these factors are expected to vary as the LASA is updated, a meritorious design feature would be a programmable format translator. The advantages of such an interface concept should be comprehensively weighed when considering the slightly increased instrumentation complexity.

A complete history of the LASA instrumentation output and mode should be made available to the recording equipment so that all pertinent data is retained, thereby enabling the re-creation of array observations with a fidelity limited only by the field equipment. However, a variable magnitude scaling and sample rate for presentation to the detection processor is desirable to permit the simulation of degraded field instrumentation so that design trade-off data could be conveniently obtained and/or verified.

C.4.2 System Monitor Requirements

Supervision of a system as intricate in equipment and concept as the LASA data distribution and processing complex must be based upon timely data with an adequate display of the system status and performance. Consideration of these essential system monitoring requirements at an early stage of design can result in an efficient and orderly integration of the equipment required for the system supervisory function. Figure C-2 portrays a data monitor and crosscheck capability for event detection which is consistent with the envisioned subarray electronics configuration and utilizes the inherent flexibility of computer-driven display technology.

Diagnostics can be performed on the analog instrumentation by inserting signals of known characteristics at various points throughout the system. Fault detection and localization can be accomplished by this technique. Channel calibration is facilitated by a Proof-Mass Torqueing capability which superimposes disturbance forces at the transducer. When a broadband disturbance of known waveform is applied, the amplitude and phase characteristics of the channel can be estimated as a function of frequency. This channel signature will be very valuable in detecting component drift as a part of system diagnostics.

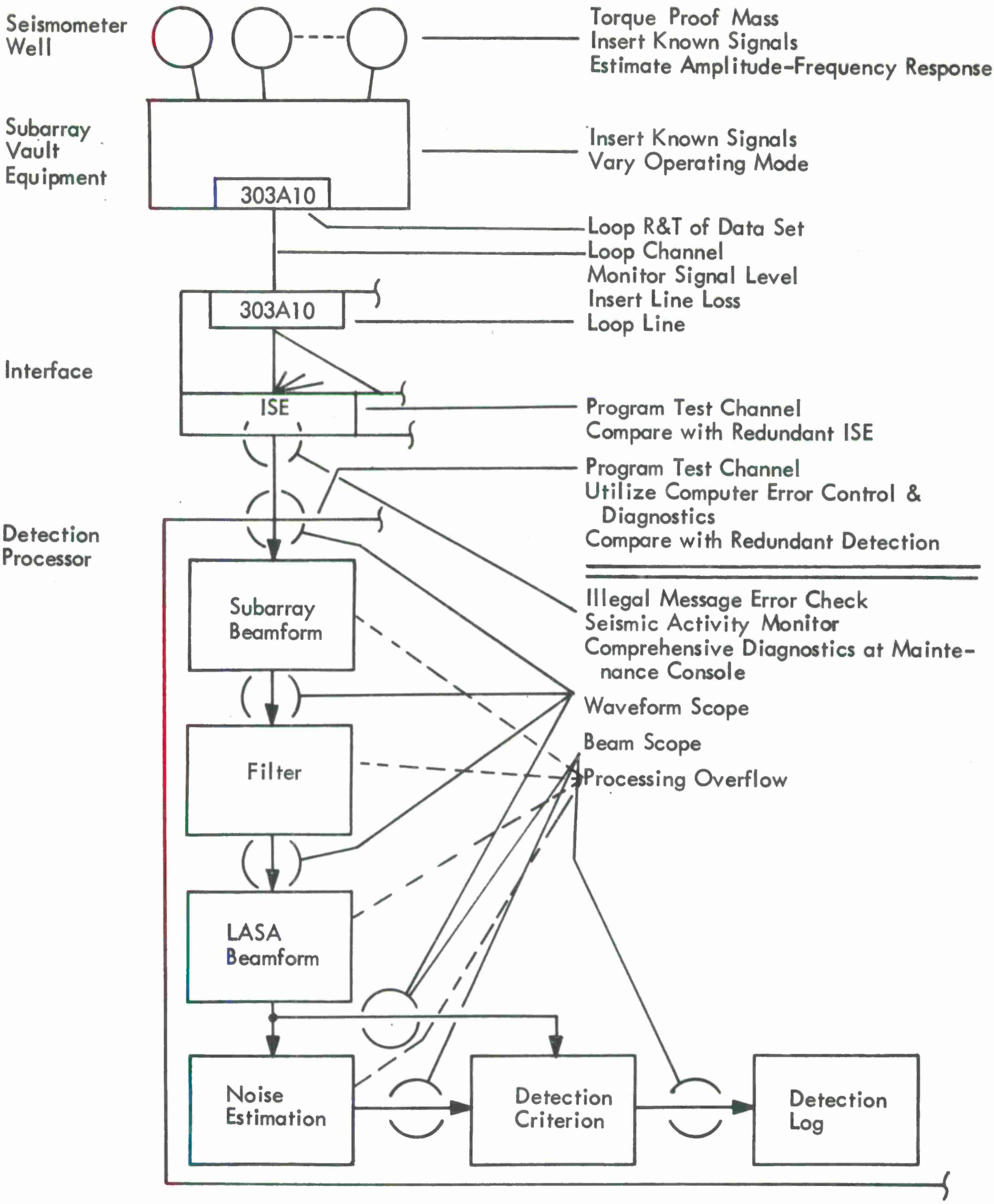

Figure C-2. Data Monitor and Cross-Check Capability

Localization of faults in the subarray vault equipment is presently based on signal substitution or superposition through mode controls, and on the monitoring of diagnostic variables such as temperature and key voltages. Because a good portion of this equipment is digital, the inclusion of conventional digital diagnostic operations appears advisable.

The telephone gear is well instrumented for communication diagnostics, and the details can be found in Bell literature. In essence, it is based on the capability to loop the channel at numerous points and to insert artificial line losses into the channel. Coordination of these tests with the LASA system is beneficial to both operations and diagnostics.

After multiplexing, a convenient monitor tool is the test channel which serves as a performance standard. Inputs to this channel may be deterministic or live data. The output derived from a deterministic input is easily checked, and provides a means to verify the process. Obviously, an on-line channel cannot be checked by this technique, and a multiplexed parallel channel utilizing live data may be necessary if undisturbed operation is essential during diagnostic operations.

General-purpose digital computers are provided with a comprehensive diagnostic and error control system. Internal parity, format checks, processing overflow detection, and the normal periodic off-line diagnostic operations adequately support the maintenance function. However, an on-line monitor capability is desirable to present that data necessary for system supervision.

Data for the LASA processing system is acquired from over 500 seismic instruments. Though each instrument is not an indespensible source of intelligence, each should be monitored to assure timely detection at a failure in the signal integrity. A seismic activity monitor as a continuous input monitor is suggested to create confidence in the input data and to illuminate questionable channels so that they may be referred to the maintenance queue for detailed performance analysis. It is inconceivable that this broad monitor function could efficiently display all maintenance and documentation provisions, but rather that it should be a comprehensive indicator of the channel status.

A requirement exists to simultaneously display selected waveforms to portray the signal signature, to verify multi-arrivals from a single event, and to serve as an editing table for that data which is selected for hard copy. An observer will be able to verify proper system operation and participate in the refinement of arrival time interpretation. Input parameters, amplitude scaling, and time scaling must be selectable by the operator. An adjustable time base for each trace is desirable to enable independent waveform sliding for efficiency analysis of multi-arrival events. This implies a memory requirement sufficient to store each significant return from a single event. Cursor measurements can be compensated to ensure true time readings.

Much of the processed data has geometric significance in "K-space." Portrayal of this intelligence requires a third display dimension which can be efficiently encoded as intensity modulation of a two dimension field. Because a large dynamic signal level is encountered, some method of data compression may be desirable. Decision theory suggests logarithmic data compression, and this technique has found wide acceptance in radar display technology. A calibrated pedestal and a selectable display range are two other features which may be interpolated from the extensive information retrieval experience accumulated by the radar industry.

A resolution of 0.5 db is desired to conveniently verify LASA beam patterns. Figure C-3 illustrates the logarithm quantum as a variable number of significant binary digits are interpreted. The required display resolution does not materialize when five or fewer digits are considered. Note that a 6-digit algorithm would result in a 2nd quantum which is nearly 2.5 times the 6th quantum, and would produce an irregular display. Consistency within 10 percent of the normal value is obtained when a 7-digit algorithm is employed. This design selection is considered optimum for the LASA System.

System maintenance and operation will involve console features beyond these monitor displays. A digital input and output will be required to insert and display operational parameters. Numerous requirements for discrete indicators of status and discrete control of modes will evolve as the study progresses. Documentation facilities must be carefully configured to efficiently generate the essential hard-copy

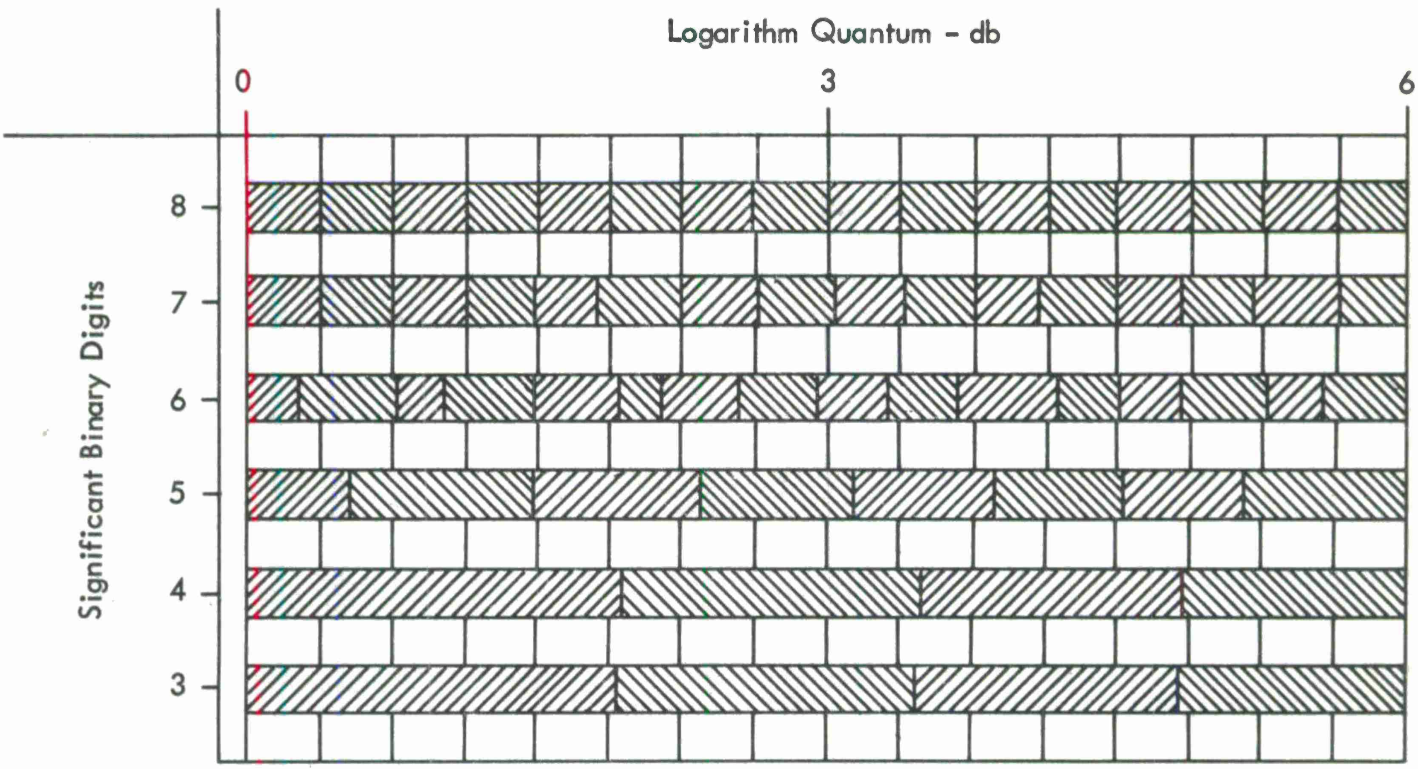

Figure C-3. Logarithm Quantum vs Significant Binary Digits

histories without burdening the facility with excessive logistic or storage requirements. Much additional effort must be applied in this area to define a smoothly functioning and well integrated facility.

C.5 RELIABILITY ANALYSIS

In the First Quarterly Technical Report* a system was presented. The primary detection mode of operation required the detection processor to continually perform the detection process and record seismometer tape. The event processor would perform this function when the detection processor was inoperable.

Of interest is the reliability achieved in such a configuration. Consider the system shown in Figure C-4. The system receives data from 21 LASA subarrays for processing. For purposes of this analysis, a failure is the loss of detection processing capability. The minimum requirement for detection processing is a continuous path through the reliability model shown in Figure C-5 to a minimum of three tape drive units. This allows an event to be detected and an input tape for event processing to be written. The reliability analysis model can be considered as a cascade of four independent submodels, each of which is required for detection processing. Therefore, the reliability of the total system model is the product of the reliabilities of the four submodels.

Systems with redundant units which can be repaired without disrupting the system performance must be analyzed by techniques which consider the effect of repair on the effective system functional reliability. One method of approaching the problem is to employ a Markov process describing the complex system relations by the transitions or relationships between discrete states defined as system parameter analogs. In reliability analysis, a state of the system would be described by the operating condition of the subunits. As an example, a system with two units could be described by the four states in Table C-1.

---

*IBM, First Quarterly Technical Report, "LASA Signal Processing and Communications Study," Contract No. AF 19(628)-5948, May 27, 1966.

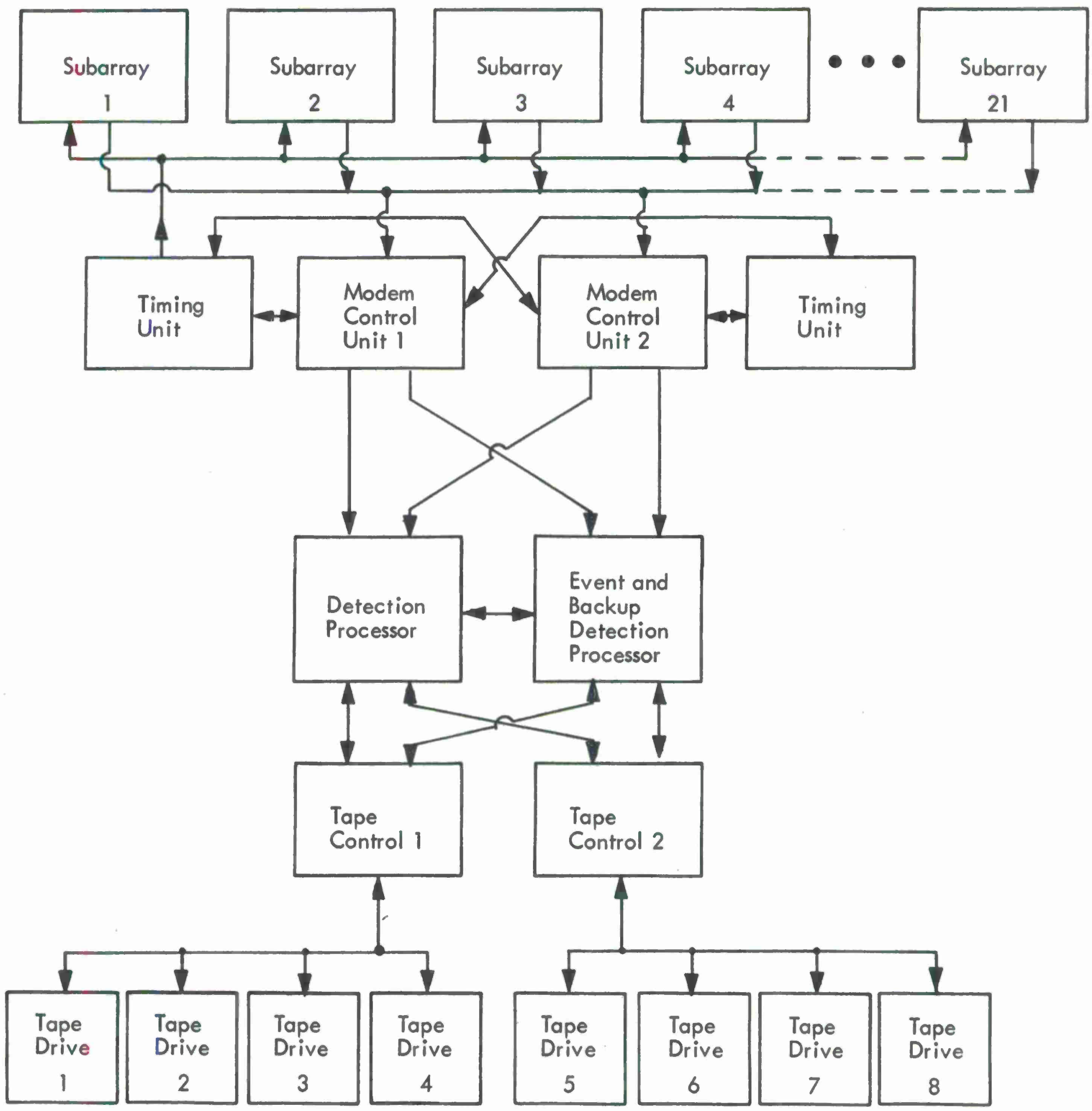

Figure C-4. Initial LASA Data Processing System Signal Flow Diagram

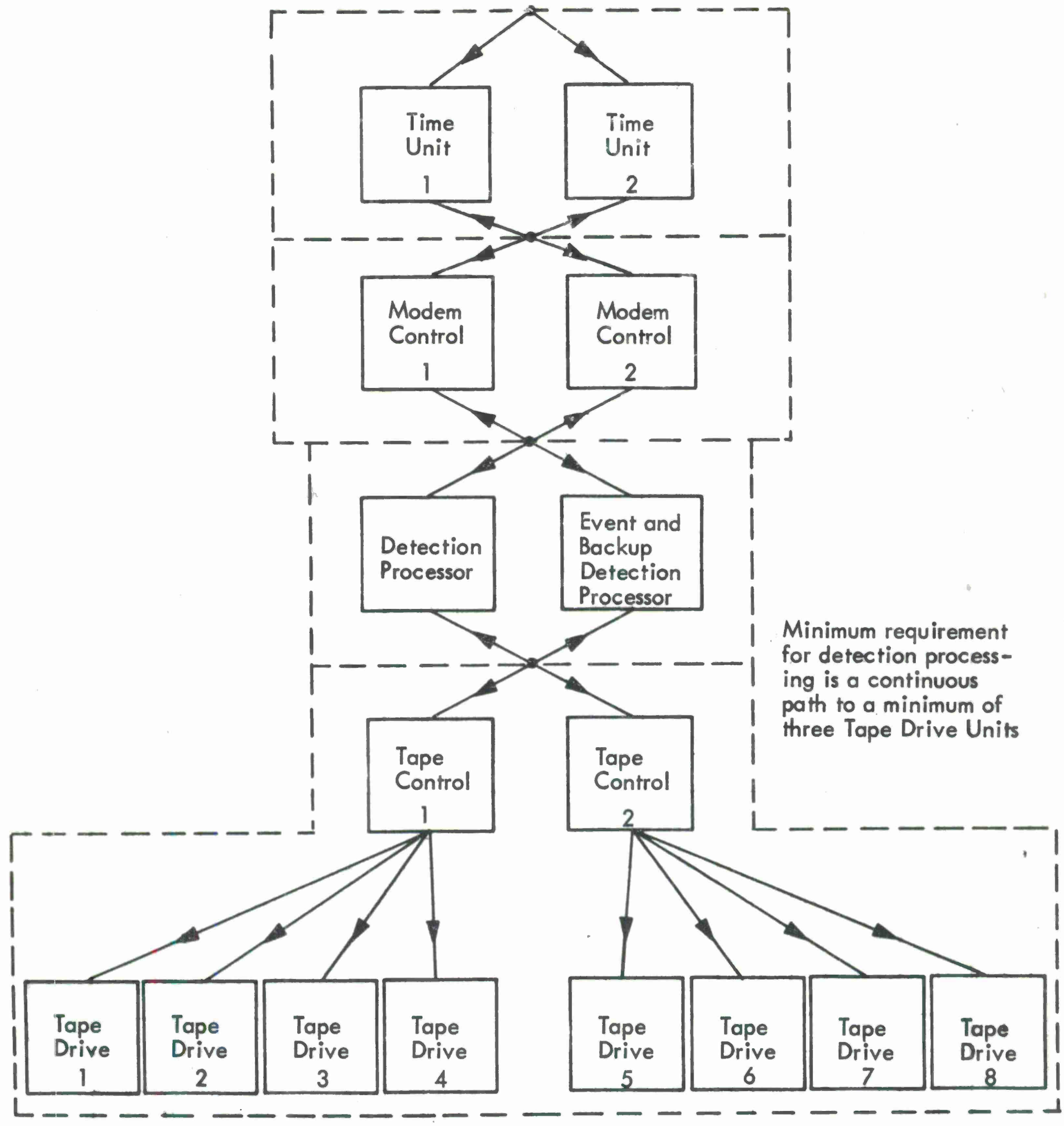

Figure C-5. Reliability Analysis Model for Initial LASA Data Processing System

Table C-1. Two-Unit Operating States

State	Unit 1		Unit 2	
	Operational	Inoperative	Operational	Inoperative
1	X		X	
2		X	X	
3	X			X
4		X		X

Whether the system is operational for each state would depend upon the configuration of the units (cascaded or parallel). Extending this to a system with n number of units, the total number of states would be two raised to the n^{th} power. However, only the states defining an operational system need be considered. All of the other states describing a failed system can be grouped together as one inoperative state. It is assumed that two failures will not occur at the same instant of time thus limiting transitions to branches between states differing by a single failure. Figure C-6a shows the flow graph for the four states of a two-unit system. All four states would be of interest only for the case of two units being in parallel. At analysis time equal to zero, both units are assumed operational. The initial value at the node corresponding to state 1 would be unity and the initial values at all other nodes would be zero. The signal flow graph can be manipulated to produce the configuration shown in Figure C-6b when both units have the same values of MTBF (Mean Time Between Failure) and MTR (Mean Time of Repair).

The potential at each node represents the probability of the system being in the state represented by the node. Therefore, one minus the potential as a function of time at the node representing the failed state gives the probability of successful system operation as a function of operating time.

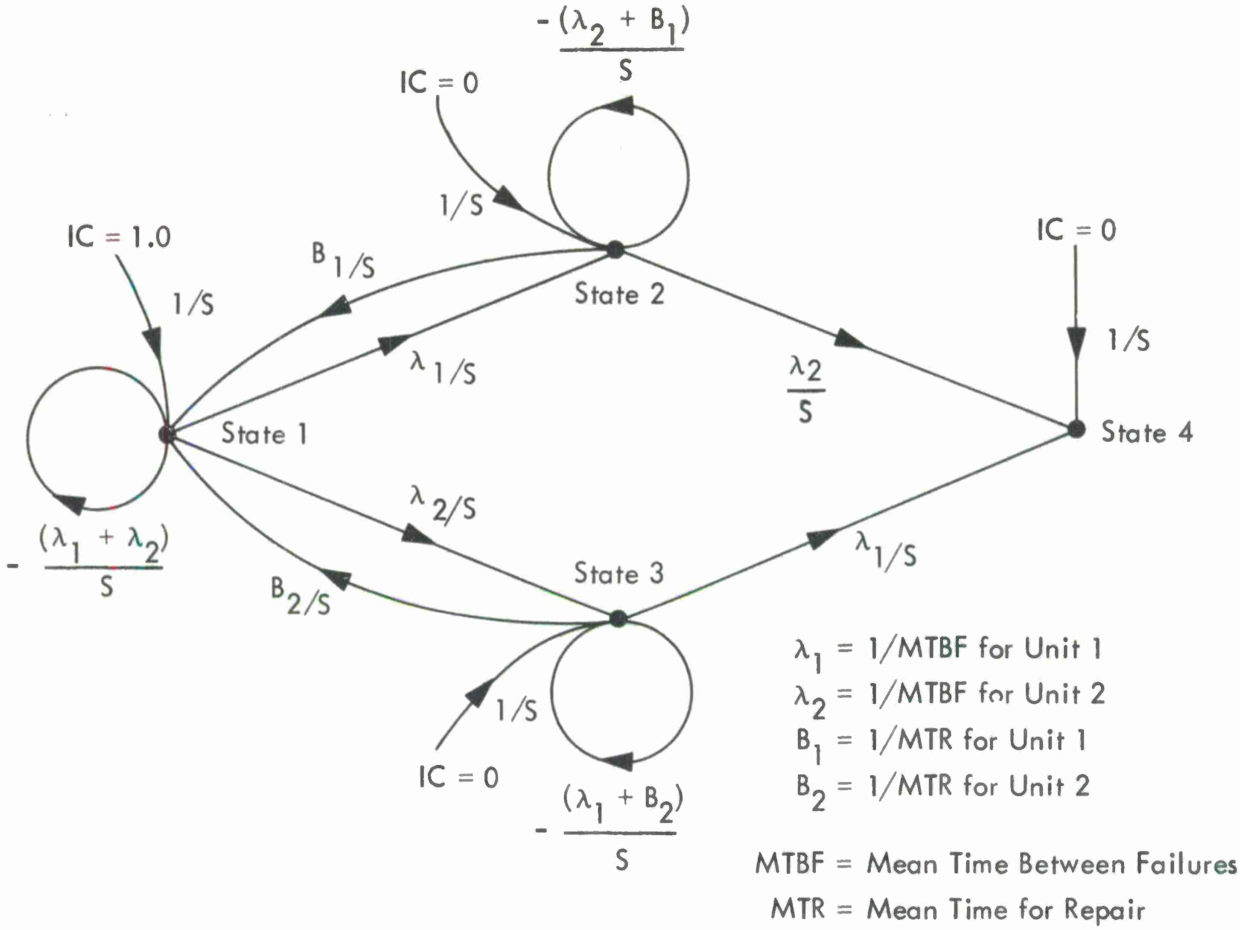

a. Two-Unit System

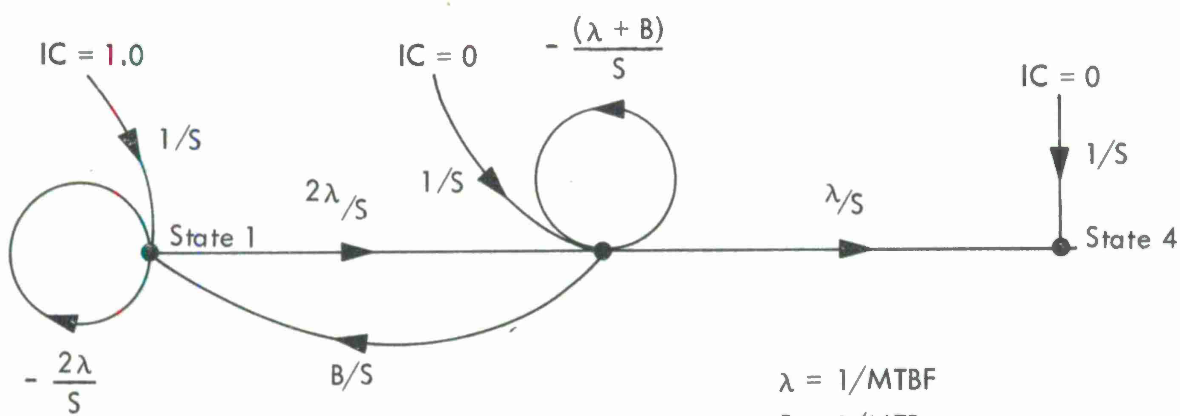

b. Two-Unit System with Units in Parallel

Note: Figure C-6a reduces to Figure C-6b for two units with equal values of MTBF and MTR operating in parallel.

Figure C-6. Reliability Flow Graph for Two-Unit System

Using typical representative assumed values of MTBF and MTR, the probability of successful uninterrupted processing as a function of operating time was calculated for the system configuration shown in Figure C-4. The probability of successful system operation for 100 hours with and without repair is 0.958 and 0.830, respectively, and for 200 hours, 0.914 and 0.557, respectively. The marked improvement in system operation with repair indicates the need for both scheduled preventive maintenance as well as "on-call" maintenance.

Appendix D

COMMUNICATION STUDY

Data transmission represents a significant fraction of the LASA system functions. The 19.2 Kbs data rate from each of the 21 subarrays generates a serial 403.2 Kbs data rate when multiplexed onto a single line. Due to the redundant bit coding used in the subarrays, the composite information rate is one-half this data rate, or 201.6 Kbs. In this appendix, the transmission of LASA data from a collection point to a remote signal processing center, and certain trade-offs that may be relevant in reducing the data transmission load, are addressed. In addition, some comments on message framing and error encoding techniques pertinent to the long-line transmission techniques are included.

D.1 DATA TRANSMISSION

To provide an estimate of the costs involved in data transmission, a specific case of transmitting LASA data from the present Billings, Montana facility to a signal processing center located in the Washington, D. C. area was examined. Although several locations were considered, only one is presented here to exhibit method of analysis and trade-off variables. Two approaches were considered. The first assumed that data must be transmitted automatically and in real time. The second assumed that the fixed delay inherent in shipping the data via air freight was acceptable. In both cases, the costs involved in acquiring the data have been omitted because the added cost of the tape writing operation is approximated by the cost for an added unit between the modem and the remote signal processing system.

The Commercial Communication Rates for equipment covering the range of bandwidths of interest are presented in Table D-1 and the costs for manual data transmission are presented in Table D-2. Using Tables D-1 and D-2, the automatic data transmission cost compares favorably to the manual method for data rates accommodated by both the TELPAK A and TELPAK B. Without attaching any economic significance to the fidelity, reliability and convenience of the automatic method over the manual method, an additional trade-off variable of distance between the remote processing site and the central collection point can be examined. Because most of the cost is a direct function of distance, the cost break point in favor of TELPAK C and D exists for tariff mileages less than 1333 and 725, respectively.

The data rate at Billings would require a TELPAK D system, however, the useful information rate can be accommodated by a TELPAK C. Because TELPAK B exists physically as two TELPAK A's operated in parallel, its utilization introduces complicating control problems. Therefore, efforts to reduce data rates below TELPAK C capability have been aimed at fitting within a TELPAK A channel.

Three variables have been considered in trade offs aimed at reducing the data rate:

a. Sampling Rate—The current 20 Hz sampling rate appears excessive with respect to the anticipated signal frequency and further analysis may verify that a 10 Hz sampling rate is adequate. This, combined with the reduction in redundant bits permitted by polynomial coding for message framing and error checking, allows use of 100 Kbs channels.

b. Number of Words per Subarray—The 32 words received from each subarray, each sample period, presently contain only 26 words of interest in beamforming. In addition, current simulation processing casts doubt upon the usefulness of the inner ring of six seismometers per subarray, offering further potential reduction in the number of words to be transmitted.

Table D-1. Commercial Communication Rates

	Kc	Kbs	$/mile	$/Month Two Terminals	One-Time Installation/2
Voice Line	4	2.4	$ 2.02 1st 150 1.717 to 500 1.616 over 500	$50	$20
TELPAK A	48	50	15.00	680	500
TELPAK B	96	100	20.00	1360	1000
TELPAK C	240	230.4	25.00	1890	1000
TELPAK D	480	500	45.00	2600	1800

Monthly Costs, Billings to Washington.

Tariff Mileage = 1631 miles

	Voice Line	TELPAK A	TELPAK B	TELPAK C	TELPAK D
Mileage	$2,950	$24,500	$32,600	$40,800	$73,395
Terminals	50	680	1,360	1,890	2,600
Total Monthly	$3,000	$25,180	$33,960	$42,690	$75,995

Note: A recent U. S. Appeals Court decision has ordered AT&T Corp. to make TELPAK A and B rates correspond to private line rates and to increase TELPAK C and D rates. Major TELPAK users have asked for a stay of this order until they can carry an appeal to the Supreme Court. Ultimate effect of this litigation on TELPAK rates is uncertain at this time.

Table D-2. Data Transmission Costs by Tape
(Billings, Montana to Washington, D. C.)

Assumptions

a. Operation is 24 hours per day and 7 days per week.

b. 800 BPI, 3 characters per word format yielding 160 tapes per day.

c. All operations done in parallel with present recording activity.

d. CPU time is available to write second tape.

		Purchase	Monthly
1.	Tape Control Unit	$18,900.[1]	
2.	Two Tape Drives	60,800.[1]	
3.	Montana—two operators per shift @ $1300 per man month		$11,700.
4.	Air Freight @ $53 per 100 lbs.		10,812.[3]
5.	Washington—two operators per shift @ $1300 per man month		11,700.
6.	Tape inventory, 1600 reels @ $33.50 per reel	53,600.[2]	
7.	Estimate Maintenance Cost		1,000.
		$133,300.	$35,212.

1. Equipment catalog costs.

2. Costs from IBM Authorized Federal Supply Schedule Price List dated January 17, 1966 for 800 BPI tested tape IBM P. N. 339269.

3. Air freight costs based on 4.25 pounds per tape reel and $51 round trip air freight with $1 ground handling at each terminal for each 100 pounds shipped.

c. Word Size—Work is now in progress to determine the necessity or desirability of carrying the full 13 bit plus sign quantization of the data words. In addition, it has been shown that, for low signal-to-noise ratio, beam forming with infinitely clipped signals results in negligible loss.*

A subarray message configuration which may be worthy of consideration uses 19 words for short-period instruments, three words for long-period instruments, three for environment sensors, one control word, and two spares. Using Figure D-1, it can be shown that employing a 28-word message allows 8 bits per word at 10 Hz in a TELPAK A.

D.2 OTHER CONSIDERATIONS

For long-distance transmission, it appears necessary to not only provide message framing but also error detecting. The Start of Message word for message framing and simple word parity of the present system utilizes approximately 10% of the available data bits and is not particularly effective for the burst and dropout errors that are characteristic of long-line communication links. An alternate approach would be to utilize a polynomial coding** as an efficient means of providing simultaneous error coding and message framing. Assuming that data is transmitted in 1000 bit messages, a 28-bit polynomial code has been selected for message framing and error checking. This represents only 2.8% redundant bits for both functions, providing a strong message framing capability and virtually eliminating undetected transmission errors.

---

*V. C. Anderson, "Digital Array Phasing," Journal of the Acoustical Society of America, Vol. 32, No. 7, 1960.

*P. Rudnick, "Small Signals in the DIMUS Array," Journal of the Acoustical Society of America, Vol. 32, No. 7, 1960.

**A. H. Frey, Jr., "Message Framing and Error Control," IEEE Transactions an Military Electronics, Vol. MIL9, No. 2, April 1965.

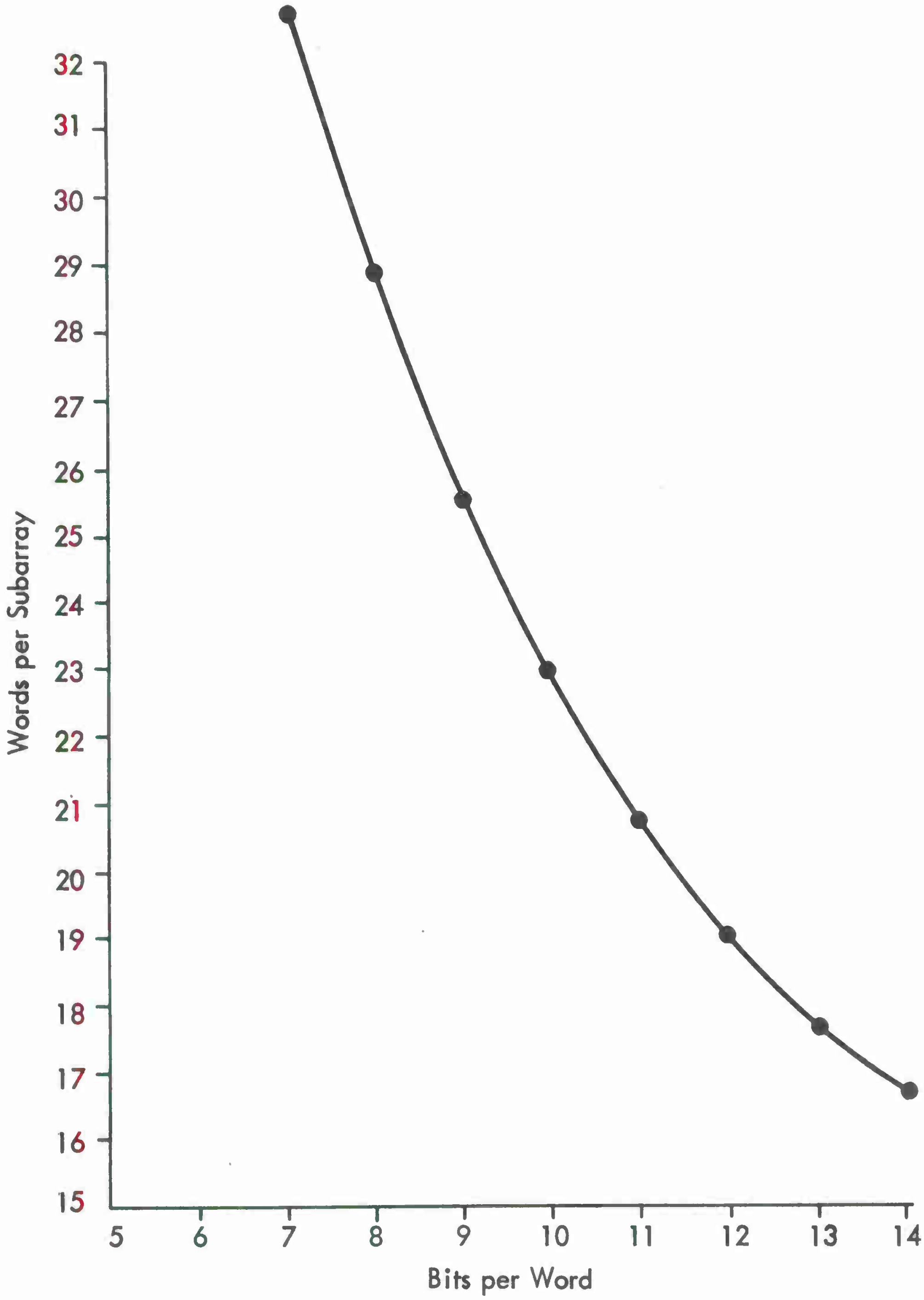

Assumptions:

a. Available channel is 50 kbs, TELPAK A.
b. Messages are 1,000 bits long.
c. A 28-bit polynomial is used for message framing and error detection.
d. Sampling Rate = 10 Hz.

Figure D-1. Word Size vs Number of Words

The specific 28-bit polynomial was generated in the following manner: The first two irreducible polynomials of degree 10 in Peterson's Tables were multiplied together to obtain a polynomial of degree 20. This polynomial is then multiplied by $X^3 + 1$ and $X^5 + X^2 + 1$ to obtain the resulting 28th degree polynomial: $X^{28} + X^{23} + X^{20} + X^{19} + X^{15} + X^{14} + X^{11} + X^{10} + X^8 + X^4 + X+1$.

The polynomial code thus formed has a minimum distance of 6, ensuring detection of all error patterns comprising five or fewer erroneous bits, regardless of location in the message. The incorporation of the factor X+1 (in $X^3 + 1$) ensures that all patterns with an odd number of errors will be detected. The error detection capability can be summarized as follows:

a. All error patterns containing five or fewer errors in the message are certain to be detected.

b. All single bursts of error of duration less than 29 bits are certain to be detected.

c. Of the error patterns with six or more errors, all patterns with an odd number of errors will be detected.

d. Error patterns with six or more bits in error will be detected with a probability approximately equal to 1 minus the quantity 2 raised to the minus 28th power $(1-2^{-28})$.

Based on the error data given by Fontaine and Gallager* for voice band channels, an undetected error for the Bell A-1 modem would occur on the average of once every 18.5 thousand years. Although data is not available for the Bell 303A series of modems utilized with the LASA arrays, somewhat comparable results would be anticipated and undetected errors can be expected to be of no consequence.

Implementation of the encoding and decoding of such polynomials can be done in a general purpose computer, but not very efficiently.

---

*Fontaine and Gallager, "Error Statistics and Coding for Binary Transmission Over Telephone Circuits", Proceedings of the IRE, June 1961.

Special polynomial encoder-decoders have been built, however, that efficiently implement this operation. As an example, the encoding and decoding logic for the polynomial $P(X) = 1 + X^2 + X^4 + X^5$ is shown in Figure D-2.

For encoding, the message enters the input of the shift register to generate the five polynomial bits as indicated in the logic. The AND gate, A_1, is closed to allow the feedback through the EXCLUSIVE OR gates as the five redundant bits are generated. Simultaneously, the message is fed through the five-bit delay to the output. After all data bits plus five zeros have been shifted in, the remainder in the register constitutes the five redundant bits. AND gate A_1 is then opened and AND gate A_2 closed and the five redundant bits sent out at the end of the message. Decoding operates in the same manner, with the error check for zero after the received message and the redundant bits have been put through the register.

To incorporate message framing, a message length buffer is added because the receiving end does not know where the start of a message is until it has received the entire message with its redundant bits and completed the polynomial check. In effect, the register looks at the last N bits where N is the total message length (data plus redundant bits), to determine if a valid, error-free message exists. Thus, the data is continually scanned for valid messages through a sliding window, N bits long.

In this type operation, one other addition must be made. Because equipment is always looking at the last N bits to see if it is a valid message, it does not want to be biased by earlier bits. Therefore, after N bits have been shifted through the register, when the N + 1 bit is shifted in, the first bit is fed back into the register to cancel its effect on the running value in the polynomial register. In this way, for both encoding and decoding, the register always contains the value corresponding to the last N bits that have gone through it. In actual implementation, other features, such as a nonzero check value, may be added to guard against the more common catastrophic failure conditions.

The value of the above type of error detecting lies not only in the protection it gives the signal processing system from transmission noise, but in the strong diagnostic aid it provides for fault conditions. Because for all practical purposes, the undetected error rate is zero, such a system allows immediate isolation of the transmission line as a fault source.

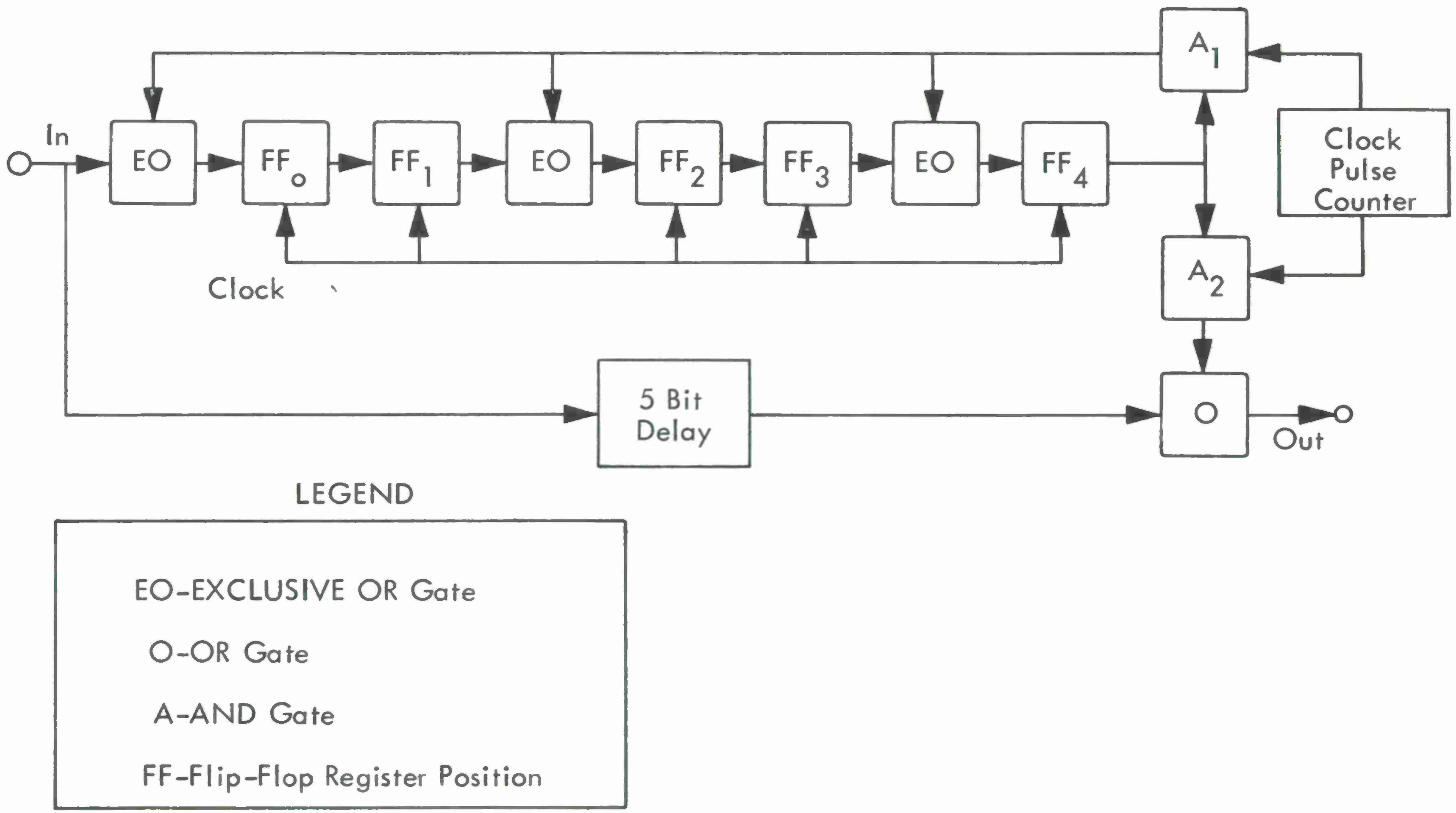

Figure D-2. Coding Logic

Appendix E

DATA ANALYSIS PROGRAMS

E.1 INTRODUCTION

This appendix presents a general description of the Data Analysis Programs being developed.

For the most part, all the programs discussed are operational in the sense that a working model of each program is available. Most of the programs, however, are not complete and changes are being made either to increase their capability in a general sense or to modify them to the individual characteristics of a particular experiment.

The programs are generally written in FORTRAN IV so that they are easily adaptable for processing on different machines. The majority of the programs are currently being executed on an IBM 7090 although some are specifically written for the IBM System/360. The input routines for the LASA Tape Edit and Subarray Beamformer programs are written in IBM 7090 MAP language and must be rewritten in System/360 Assembler Language prior to conducting experiments on the System/360.

E.2 LASA TAPE EDIT

E.2.1 Purpose

The LASA Tape Edit program converts LASA raw data tapes into FORTRAN compatible binary tapes. Any or all 651 channels or any portion thereof may be selected for editing.

E.2.2 Description

E.2.2.1 Input

Program input consists of edit processing control cards and from one to three LASA raw data tapes.

The control cards are used to indicate to the program (a) the number of records to be skipped before initiating the editing process, (b) the number of records to be edited, (c) the number of channels to be edited, (d) the number of LASA raw data tapes to be mounted and their respective names and reel numbers, and (e) the channel number of each channel to be edited.

Each LASA raw data tape is a low-density (556 BPI) tape with each data word being 18 bits in length with extended sign and odd parity. Negative numbers are in two's complement notation. A record on a raw data tape consists of: (a) a four-word header containing the date-time data, (b) two frames each containing 651 words representing one data sample from each of the 651 channels per time interval of 50 milliseconds, and (c) a seismometer status trailer when required. All trailer data is ignored during the editing process.

E.2.2.2 Computation

Each record on the raw data tapes is unpacked and placed in individual IBM 7090 words. The data channel values (seismometers) are converted to true floating-point notation. The data is then arranged in memory for subsequent recording.

E.2.2.3 Output

Program output consists of an off-line printout and as many FORTRAN compatible LASA edit tapes as are required during the editing process.

The off-line printout lists all the information supplied on the input control cards as indicated in Section E.2.2.1. It also contains the number of logical records on the output edit tapes, raw data tape record numbers where read checks occurred (if any), the locations of unexpected end of files on the raw

data tapes encountered prior to the completion of the specified number of records to be edited, and data from the header record written on the first LASA edit tape as described below.

Each LASA Edit tape is a high-density (800 BPI) tape with each data word being 36 bits in length. Each logical record on LASA edit tape will consist of from one to 651 data words. Because these logical records are written in FORTRAN, each will be subdivided into physical records of no more than 256 words. The first logical record is a header record which contains in consecutive word order the year, day, hour, minute, second, and millisecond of the first data sample record which follows the header, and the number of edited channels and their respective channel numbers. The header words are in fixed-point form. Each logical record which follows the header record consists of a floating-point data sample of all the channels selected for editing. As raw data tapes are recorded, four data samples are lost during reel switching. To compensate for these lost records, four logical records of the last available data will be recorded when an end of file is reached on all but the last raw data tape.

E.2.3 Program Interaction

The edited tapes generated by this program form the input for the Subarray Beamformer (SBF) program.

E.2.4 Program Restrictions

The program expects only one end of file per LASA raw data tape. Because LASA raw data tapes do not contain a year in their header, an NYEAR = card must be inserted in the "Read I Subroutine." The present deck has a NYEAR = 1966.

E.2.5 Comments

The LASA Tape Edit program is designed for the IBM 7090 computer under IBSYS supervision and is written in FORTRAN IV and MAP. All reading is done by Library IOCS and writing by FORTRAN IV.

E.3 SIGNAL-TO-NOISE RATIO CONTROL

E.3.1 Purpose

This program constructs a LASA data tape containing a specified number of noise samples followed by a specified number of signal samples, each of which has been multiplied by a unique scaling factor and added to a noise sample. The overall effect is the generation of a magnetic tape containing an event in which the signal-to-noise ratio can be controlled. This tape would then be available for processing through pertinent data analysis programs.

E.3.2 Description

E.3.2.1 Input

The program reads a LASA tape in edited form and extracts segments of noise samples and signal samples. Simple control cards provide the capability to precisely choose the portions of noise and signal samples to be used by the program in generating a pseudo-LASA event tape with a known signal-to-noise ratio. Scaling factors for each seismometer present on the input tape are provided by card input.

E.3.2.2 Computation

A pseudo-event tape may consist of more than one reel (4 minutes of LASA seismometer data) and may use more than one reel of input tape for its generation.

The program has the following characteristics:

a. Each channel (seismometer) must have a distinct scaling factor. If there are more channels than scaling factors, the remaining channels will be scaled by a factor of 1.0.

b. A designated number of time samples may be skipped prior to taking the noise sample.

c. A designated number of records may be skipped between the end of the noise sample and the beginning of the signal.

d. The number of noise samples must be greater than the number of signal samples. The difference will be the number of noise samples at the beginning of the output tape.

E.3.2.3 Output

Output tape(s) are written in the same format as the input tape(s) and contain the same number of channels. The first X number of records are noise samples, and the rest of the records are scaled signal plus noise.

E.3.3 Program Interaction

The input and output tapes are in the LASA Tape Edit format. Therefore, signal-to-noise ratio can be adjusted on any tapes of that format.

E.3.4 Program Restrictions

The only restriction is that enough data must be present on the input tape to accomplish the production of the signal-to-noise ratio output.

E.3.5 Comments

The program is written in FORTRAN IV and MAP for the IBM 7090.

E.4 INVERSE VELOCITY SPACE MAPPING

E.4.1 Purpose

This program prepares inverse velocity space maps of the world land areas and seismic zones as well as lines of constant geocentric latitude and longitude.

E.4.2 Description

E.4.2.1 Input

Two forms of input are acceptable: (a) pairs of latitude and longitude to be mapped into inverse velocity coordinates, or (b) initial latitude and longitude coordinates and an incremental value for each to generate coordinate lines for inverse velocity space mapping.

E.4.2.2 Computation

The transformations consist of calculating range and azimuth by means of spherical trigonometry and then converting range to horizontal phase velocity. For more detailed discussion of the computation involved in this program, see Appendix A.

E.4.2.3 Output

The output of this program consists of a printout, for each coordinate, of range, the inverse phase velocity, and azimuth; and a plot produced for the CALCOMP plotter.

E.4.3 Program Interaction

None.

E.4.4 Program Restrictions

None.

E.4.5 Comments

The program is written for the IBM 7090 in FORTRAN IV using CALCOMP plotter subroutines.

E.5 FILTER PROGRAMS

E.5.1 Coefficient Generator Program

E.5.1.1 Purpose

This program generates recursive filter coefficients for a given low-pass, high-pass, band-pass or band-reject Butterworth or Chebychev filter with the option of calculating a frequency response, an impulse response of both the filter transfer function and its denominator, and corresponding bias and variance coefficients.

E.5.1.2 Description

E.5.1.2.1 Input

The desired filter variables (type, kind, order) must be specified along with sampling rate and center and/or cut-off frequencies.

E.5.1.2.2 Output

This program gives as printout the a and b filter coefficients along with a frequency response.

E.5.1.3 Program Interaction

Filter coefficients generated by this program will be used in the recursive filter in the Subarray Beamformer (SBF) program.

E.5.1.4 Program Restrictions

Subject to precision requirements, the program is limited to order 20 for low-pass and high-pass filters and limited to order 10 for band-pass and band-reject filters.

E.5.1.5 Comments

This program is written in FORTRAN IV for 7090. The equations used in the computations are not finalized and are not presented herein.

E.5.2 Frequency Response Program

E.5.2.1 Purpose

This program generates a frequency response for a set of input filter coefficients.

E.5.2.2 Description

E.5.2.2.1 Input

The a and b filter coefficients are required as input.

E.5.2.2.2 Computation

The magnitude of the loss in db and the phase angle are calculated for a range of frequencies,

$$H = \frac{\left(a_o + \sum_{n=1}^{k} a_n \cos nwT\right) - j\left(\sum_{n=1}^{k} a_n \sin nwT\right)}{\left(b_o + \sum_{n=1}^{k} b_n \cos nwT\right) - j\left(\sum_{n=1}^{k} b_n \sin nwT\right)}$$

$$H = \frac{P - jQ}{R - jS} \qquad wT = 2\pi \frac{f_i}{f_s}$$

where:

a_n and b_n = the filter coefficients

k = the order of the filter

f_i = the frequency being investigated

f_s = the sampling rate.

The magnitude of the loss in db is expressed as

$$|H| = 10 \log_{10} \frac{P^2 + Q^2}{R^2 + S^2}$$

and the phase angle is expressed as

$$< H = \arctan \frac{PS - QR}{PR + QS}$$

E.5.2.2.3 Output

The printout consists of a range of frequencies with the corresponding db loss and phase angle for each of these frequencies.

E.5.2.3 Program Interaction

None.

E.5.2.4 Program Restrictions

The program has been restricted to a maximum of 20 filter coefficients.

E.5.2.5 Comments

The program was written in FORTRAN IV for the IBM 7090.

E.6 SUBARRAY BEAMFORMER (SABF)

E.6.1 Purpose

This program produces a variable number of subarray beams for each subarray considered. In addition, the option to pass the beams through a digital filter is also available. The purpose of the program is to produce unfiltered and filtered subarray beams which will be used for further processing.

E.6.2 Description

E.6.2.1 Input

LASA edited tape(s) is the main input to the SABF program. This input represents the data from a selected number of seismometers for a selected period of time. The number of seismometer channels recorded on the tape dictates the number of elements in each beam sum. An equal number of seismometers from each subarray must, however, be present on the tape.

In addition to the seismometer data, digital filter parameters and time delays form the other input data.

E.6.2.2 Computation

There are three main computations present in SABF: beamforming, filtering, and thresholding.

E.6.2.2.1 Beamforming

The following equation represents the computation involved in the process of beamforming in SABF:

$$B_{jk}(t) = \frac{1}{I} \sum_{i=1}^{I} f_{ij}(t - n_{ijk})$$

where:

I = number of seismometers

j = j^{th} subarray

k = k^{th} beam

t = current time sample

n_{ijk} = time delay for the i^{th} seismometer in the j^{th} subarray, for the k^{th} beam

f_{ij} = LASA raw data from the i^{th} seismometer in the j^{th} subarray

$B_{jk}(t)$ = resultant subarray beam for the k^{th} beam in the j^{th} subarray.

As indicated in the equation, each beam formed represents a delayed sum of a set of seismometers from a particular subarray. This process is repeated, using a different set of time delays, for each beam formed in that subarray, and then repeated for the total number of subarrays present. The number of beams formed, then, is j times k, with each beam formed by summing I properly delayed seismometers. The variables I, j, k, as well as the data, f_{ij}, and time delays, n_{ijk}, are provided as input to this program.

E.6.2.2.2 Recursive Filtering

The following equation represents the computation involved in the process of recursive filtering in SABF:

$$G_{jk}(t) = \sum_{p=o}^{P} a_{jk}(p) \cdot B_{jk}(t-p) - \sum_{p=1}^{P} b_{jk}(p) \cdot G_{jk}(t-p)$$

where:

P	=	the order of the filter
j	=	j^{th} subarray
k	=	k^{th} beam
t	=	current time sample
$a_{jk}(p)$	=	filter coefficients
$b_{jk}(p)$	=	filter coefficients
$B_{jk}(t-p)$	=	the k^{th} beam formed in the j^{th} subarray at sample time (t-p)
$G_{jk}(t-p)$	=	the k^{th} filtered beam formed in the j^{th} subarray at sample time (t-p)

As the equation indicates, the filtering is performed on the beams formed in SABF. Each beam formed is passed through the same digital filter and a resultant filtered beam value, $G_{jk}(t)$, for the current time period is produced. The variables P, j, k, a, and b are provided as input to this program.

E.6.2.2.3 Thresholding

Each beam and filtered beam formed in SABF is compared with a threshold value provided as input to this program to determine when the threshold is first exceeded. This information is required by other programs.

E.6.2.3 Output

There are two forms of output generated by SABF: magnetic tape and printer.

E.6.2.3.1 Magnetic Tape

A tape consisting of pertinent execution parameters and all beam and filtered beam values generated is produced for use by other programs. This tape also includes the value of the center seismometer in each subarray for each sample period considered in the processing. The logical format of the tape is presented on a sample time basis. All beams, filtered beams and seismometer values formed or selected per sample period are recorded in one logical record. The total number of logical records is equal to the rate at which the beams are formed.

E.6.2.3.2 Printer

Hard-copy results of this program include such pertinent run parameters as event identification, seismometers considered, the number of samples processed, the number of beams formed, the time delays used in beamforming, filter parameters used, and the points at which the beam and filtered beam values exceeded the threshold. An option is also available to print the seismometer and beam values obtained throughout the process.

E.6.3 Program Interaction

This program requires a LASA edited tape generated by the LASA Tape Edit program. The filter coefficients used are obtained from the results of the

Filter programs. Finally, the time delays used are provided by the Threshold Time Delay program. The magnetic tape output of this program serves as input to the LASA Beamformer (LBF) program and also to the SABF Power Analysis program. The points at which the thresholds are exceeded are also used by both of these programs.

E.6.4 Program Restrictions

Data restrictions imposed on this program are as follows:

Maximum number of seismometers per subarray ---------	25
Maximum number of beams formed per subarray ---------	6
Highest filter degree ----------------------------------	6
Maximum time history of seismometers (sample periods) --	21

The above data restrictions can be circumvented for individual computer runs if trade-offs with other data restrictions prove effective.

The program requires that the number of seismometers present on the input tape be in the same sequence as they appear on the raw data tapes.

E.6.5 Comments

This program is written in FORTRAN IV except for a subroutine which reads the LASA Edit tape. This read routine is written in MAP. The program currently runs on the IBM 7090 under control of the IBSYS monitor. Possible changes to this program include the following:

a. Provide capability to vary the sampling period
b. Provide a filter on the seismometer data prior to their use in the beamformer.
c. Provide ability to process subsets of the seismometers present in each subarray
d. Provide ability to eliminate any individual seismometer in the processing.

E.7 LASA BEAMFORMER (LBF)

E.7.1 Purpose

This program forms a central LASA beam and its associated neighboring beams. The beams formed by this program will then be available for further processing.

E.7.2 Description

E.7.2.1 Input

The output tape generated by the Subarray Beamformer program (SBF) containing both unfiltered and filtered beam values is the main input to this program. In addition to this beam tape, the time delays required to form the central beam and the neighboring beams for both unfiltered and filtered beams are supplied by card input.

E.7.2.2 Computation

The beamforming process performed by this program is the same as the SABF beamforming process except that instead of the time delayed sum of seismometer data, the LASA beams are formed by a time delayed sum of subarray beams. This process is performed first for the central beam and its neighboring beams using unfiltered subarray beams as the inputs, and then for the central and neighboring beams using filtered subarray beams as the inputs.

Additional processing provides the sample period of time in which each of the LASA beams formed exceeds a prescribed threshold.

E.7.2.3 Output

This program produces a tape of LASA beams formed over a selected period of time. The logical format of the tape is presented on a sample time basis. All beam and filtered beams formed per sample period are recorded in one logical record.

E.7.3 Program Interaction

The subarray beam input to this program will be supplied by the output tape generated by the SABF program. The time delays for the neighboring beams will be supplied by the Neighboring Beams Time Delay Calculations program.

The output of this program, the LASA beam tape, will serve as input to the LBF Power Analysis program and will also be used in the LASA Beam Pattern Display process.

E.7.4 Program Restrictions

At the present time, the total number of beams this program can form is restricted to 160. The maximum time history for each beam is 325 sample periods.

E.7.5 Comments

The program has the option to form either unfiltered or filtered LASA beams or both. The type of LASA beam, filtered or unfiltered, is determined by the type of subarray beam used in the beamforming process (filtered or unfiltered). No filtering is done in the LBF program.

The program is written in FORTRAN IV for the IBM 7090.

E.8 NEIGHBORING BEAM TIME DELAY CALCULATIONS

E.8.1 Purpose

This program generates a set of time delays to form a close-packed system of beams in relation to a particular central beam being investigated.

E.8.2 Description

E.8.2.1 Input

The main input to this program is the location of the source of the event undergoing analysis which is approximated by the location in inverse velocity

space of the centerline of the best detection beam, and the arrival time of the wavefront of this event at a set of known locations (e.g., the center seismometer in each subarray of LASA).

E.8.2.2 Computation

A set of neighboring beams related to the centerline of the detection beam is defined by causing (U_x, U_y) to increment so as to form neighboring beams, and limiting the neighborhood by prescribing that

$$\left[(U_x - U_{xc})^2 + (U_y - U_{yc})^2\right] \leq R^2$$

where:

(U_{xc}, U_{yc}) = the centerline location of the detection beam in inverse-velocity space

R = the radius of the circle of the selected area of detection beam uncertainty.

A closed-packed system may be defined by incrementing (U_x, U_y) according to the rules:

$$U_x = U_{xc} + r\sqrt{3}(m + 0.5\ n)$$

$$U_y = U_{yc} + 1.5\ nr$$

where r is the 3.0 db radius of an event beam in (U_x, U_y) space, and m and n are integers.

The delay at the k^{th} subarray whose center location is taken as (X_k, Y_k,) and for a beam aimed at the location (U_x, U_y) can be expressed as follows:

$$t_k = t_{kc} - (U_x - U_{xc})\,X_k + (U_y - U_{yc})\,Y_k$$

where:

$$t_{kc} = -(X_k\,U_{xc} + Y_k\,U_{yc})$$

For each neighboring beam within the 3.0 db radius of event circle, (U_x, U_y) and the corresponding time delays are recorded.

E.8.3 Program Interaction

The location in inverse velocity space of the centerline of the best detection beam, (U_{xc}, U_{yc}), is obtained from the output of the Least Squares Wavefront program. The output of this program, the sets of time delays and centerline location in inverse-velocity space for neighboring beams within the 3.0 db radius of event circle, are used by the LASA Beamformer (LBF) program.

E.8.4 Program Restrictions

The program has been arbitrarily restricted to 21 subarrays.

E.8.5 Comments

The program is written in FORTRAN IV for the IBM System/360.

E.9 POWER ANALYSIS PROGRAMS

E.9.1 Seismometer Power Analysis Program

E.9.1.1 Purpose

This program calculates both noise and signal power at the seismometer level for any particular event investigated.

E.9.1.2 Description

E.9.1.2.1 Input

The main input to the program is a LASA edited tape which includes all the seismometer channels which are to be analyzed. Additional inputs include parameters specifying the starting point and duration for both the noise and signal power analysis, and the relative event arrival times at each of the seismometers.

E.9.1.2.2 Computation

The following equation represents the computation to determine the power in the seismometer data channels:

$$P_i = \frac{1}{N} \sum_{n=1}^{N} \left[a \cdot f_i(n) \right]^2$$

where:

N = number of samples to be included in the power sum

a = scale factor

$f_i(n)$ = the value of the i^{th} seismometer at the n^{th} sample period

P_i = the power of the i^{th} seismometer.

In addition to the power calculations on an individual seismometer basis, the average power on both a subarray and LASA level is also computed. The variance and standard deviation of the seismometer data channels are also computed.

E.9.1.2.3 Outputs

The output of this program is a list of the power sums (P_i) and 10 log (P_i) for both noise and signal. The average power values described previously are also recorded along with the pertinent variance and standard deviation information.

E.9.1.3 Program Interaction

Input to this program must be a tape recorded in the LASA Tape Edit format. System gains can be determined by comparing the results of this program with the results of the Subarray and LASA beam power analysis programs.

E.9.1.4 Program Restrictions

The noise and signal intervals must be separated by one or more sample periods.

E.9.1.5 Comments

The program is written in FORTRAN IV for the IBM 7090.

E.9.2 SABF Power Program

E.9.2.1 Purpose

This program calculates noise and signal power present in the beams formed in the Subarray Beamformer program (SABF). This data may then be compared with a similar power analysis at a seismometer level and LASA beam level to indicate overall system gain.

E.9.2.2 Description

E.9.2.2.1 Input

The main input to this program is the tape generated by the SABF program. This tape includes unfiltered and filtered beam values formed for some specified period of time. Other input values include parameters indicating points at which noise and signal analysis is to begin, duration of both noise and signal power analysis, and the points at which each beam present on the tape exceeded some prescribed threshold in the SABF program.

E.9.2.2.2 Computation

The main computations in this program are the power calculations and standard deviation performed on both noise and signal portions of the filtered and unfiltered beams present on the input tape.

The following equation represents the computation to determine the power of a beam:

$$P_j = \frac{1}{N} \sum_{n=1}^{N} \left[a \cdot B_j(n) \right]^2$$

where:

N = number of samples to be included in the power sum

a = scale factor

$B_j(n)$ = the value of the j^{th} subarray beam at the n^{th} sample

P_j = power of the j^{th} subarray beam.

In addition to the power calculations on an individual beam basis, the average beam power for all subarrays present, P, is also calculated and the associated standard deviations. This process is done first for the unfiltered and then the filtered beams.

E.9.2.2.3 Output

The output of this program is a list of the individual unfiltered beam power sums (P_j) and 10 log (P_j) for both noise and signal. In addition, the average noise and signal power for the unfiltered beams with the associated standard deviation is also presented.

The same output is recorded for the filtered beams.

An optional output is provided which presents the intermediate noise power every 20 seconds and the intermediate signal power every 0.2 seconds.

E.9.2.3 Program Interaction

This program requires an SABF output tape containing subarray beam values over some specified period of time. In addition, the output of the SABF also provides data indicating the start of the event for each beam recorded on the SABF output tape.

The resultant powers calculated in this program can be compared to a similar power analysis on both a seismometer level and a LASA beam level to indicate overall system gain.

E.9.2.4 Program Restrictions

At the present time, the program is designed to process only one unfiltered and one filtered beam per subarray. The program also expects the beam input values to be contained on a single tape. The selection of the starting points for both the noise and signal analysis, as well as the duration of both, must be done with some caution to ensure that the required amount of data is present on the beam input tape.

E.9.2.5 Comments

This program is written in FORTRAN IV for the IBM 7090.

E.10 THRESHOLD TIME DELAY

E.10.1 Purpose

This program provides the approximate time delays required to form the beams in the Subarray Beamformer program. No attempt is made to seek maximum gain or to minimize losses.

E.10.2 Description

E.10.2.1 Input

The main input to this program is a selected LASA edited tape containing an event of sufficient magnitude to allow for the successful execution of the threshold logic. Other pertinent run parameters, such as the threshold value, are provided by input data cards.

E.10.2.2. Computation

The initial computation in the program is the identification of the sample periods in which each seismometer present on the input tape first exceeds a prescribed threshold. Once each seismometer has exceeded the threshold,

time delays (on a subarray basis) are obtained by computing the difference in sample periods between the time each seismometer within a subarray exceeded the threshold and the time the center seismometer in the subarray exceeded the threshold. The time delay for the i^{th} seismometer in the j^{th} subarray is:

$$TD(i,j) = THC(j) - TH(i,j) + T(j)$$

where:

THC (j) = the sample period time in which the center seismometer in the j^{th} subarray exceeded the threshold

TH(i, j) = the sample period time in which the i^{th} seismometer in the j^{th} subarray exceeded the threshold

T (j) = sample period bias for the j^{th} subarray.

E.10.2.3 Output

The sample period times at which each seismometer exceeds the threshold as well as the time delays for each seismometer relative to its associated subarray are printed. Additional run parameters are also recorded.

E.10.3 Program Interaction

The time delays generated by this program are used in the Subarray Beamformer program (SABF) to form the subarray beams.

E.10.4 Program Restrictions

None.

E.10.5 Comments

The program is written in FORTRAN IV for the IBM 7090.

Because of the occurrence of corrupt data, the thresholds may trigger thereby generating incorrect time delays.

This has proved useful in the localization of the "glitches" and the time delays are easily adjusted by investigation of the data.

E.11 SUBARRAY PLOT

E.11.1 Purpose

This program plots seismometer data from a selected subarray for a variable period of time. The resultant plot provides a visual representation of the seismometer activity during the selected period of time.

E.11.2 Description

The Subarray Plot program produces a magnetic tape for a CALCOMP digital incremental plotter. The plotter produces a graphic representation of the values of seismometers within a specific subarray over a selected period of time.

E.11.2.1 Input

Seismometer data is obtained from a LASA edited tape while control parameters and other pertinent data such as the selected subarray identification is read from cards.

E.11.2.2 Computation

The program reads the LASA edited tape for a specified period of time and extracts after each read the seismometer values of the selected subarray. The array of seismometer data obtained over the prescribed period of time is then placed on tape by the CALCOMP subroutines for subsequent plotting.

E.11.2.3 Output

Data derived from the input tape header and input cards are printed along with execution control parameters in a descriptive format to provide pertinent run documentation. The magnetic tapes produced by the program are in the prescribed format for off-line plotting on the CALCOMP plotter.

E.11.3 Program Interaction

The program requires as input a tape generated by the LASA Tape Edit program.

E.11.4 Program Restrictions

Seismometer values are read and plotted in 22-second blocks with a limit of 6 blocks (132 seconds) per plot. The capability to continue the plot is provided by additional passes through the program. The maximum number of channels (seismometers) per subarray to be plotted is 25.

E.11.5 Comments

The program is written in FORTRAN IV for the IBM 7090. Plotting is done on a CALCOMP Model 563 plotter.

E.12 DISPLAY PROGRAMS

E.12.1 Display Test Tape Program

E.12.1.1 Purpose

This program generates four tapes to check the Experimental Display. The display is described in Appendix C.

E.12.1.2 Description

E.12.1.2.1 Input

Input to the program consists only of an indication of which tape format is to be produced. A fifth possible entry requests the program to list a generated tape in a format which approximates that of the display face.

E.12.1.2.2 Computation

Based on the input, the program internally sets up and writes out the desired tape or listing. The tapes available display a complete face of a single intensity or a bar pattern consisting of all 16 possible intensities. The single intensity is incremented through eight possible values and the bar pattern is rotated vertically to show all 16 intensities on each line of the face. Both display patterns are available in both a 60-kc and a 30-kc display rate.

E.12.1.2.3 Output

The program outputs are tapes and listings as requested by the operator.

E.12.1.3 Program Interaction

This program stands alone and is independent of other LASA programs.

E.12.1.4 Program Restrictions

Only two formats can be produced. Only two display rates (60 kc and 30 kc) are available.

E.12.1.5 Comments

This program was implemented in the Assembler Language of the Basic Programming Support for the IBM System/360. It requires a machine with one tape drive, a card reader, a printer and a console typewriter. The last requirement could be removed by using parameter cards instead of operator entries.

E.12.2 LASA Beam Pattern Display Program

E.12.2.1 Purpose

The LASA Beam Pattern Display program prepares input tapes for use on the Experimental Display (see Appendix C).

E.12.2.2 Description

E.12.2.2.1 Input

Input to this program is a magnetic tape consisting of LASA beam sums. The format of the tape is defined for ease of generation by FORTRAN and ease of acceptance by this program. The tape may be either seven or nine track. Other program inputs are parameter cards to specify the action desired and address cards which place the beam sums on the display face. This technique allows input data to come in any well defined order as long as the address cards are constructed in the same order.

E.12.2.2.2 Computation

The beam sums are read and converted to display intensities through the use of a table look-up procedure. This allows a look at any range of the beam signals in detail while suppressing all other portions.

E.12.2.2.3 Output

Two outputs are generated by the program. First is a display tape which contains from 1 to 99 copies of a display sequence. The number of copies is an input parameter. The second output is a listing of selected records of the tape in a format similar to that displayed on the display device.

E.12.2.3 Program Interaction

The magnetic tape input comes from the LASA Beamformer program after a reformatting process. The address cards are produced by the Display Address Card program.

E.12.2.4 Program Restrictions

Only two display duration times (50 - 100 milliseconds) are available. Only one output tape can be produced although the input may extend over nine reels of tape, if necessary.

E.12.2.5 Comments

This program was written in Assembler Language for the IBM System/360. It is designed to operate using the Basic Programming Support System. Input requests may be stacked and tape or listing requests may be intermixed in any order.

E.12.3 LASA Display Address Card Program

E.12.3.1 Purpose

This program generates address cards for use as input to the LASA Beam Pattern Display program.

E.12.3.2 Description

E.12.3.2.1 Input

The input to this program consists of the deck of cards generated by the neighboring beam program. This deck contains the coordinates of each beam in velocity space.

E.12.3.2.2 Computation

Each beam is placed in an internal display matrix using the inverse velocity space coordinates. The first beam in sequence is placed in the center and all other beams are placed relative to it. The method employed for placing the beams creates holes in the pattern such that beams are not displayed in contiguous display positions. A compaction process is then used with the location of the center beam remaining constant.

E.12.3.2.3 Output

A punched card deck of addresses and a listing of velocity coordinates is produced. The punched cards are suitable for input to the LASA Beam Pattern Display program.

E.12.3.4 Program Interaction

The input of this program is the output of the neighboring beams program. The output of this program serves as part of the input to the LASA Beam Pattern Display program.

E.12.3.5 Program Restrictions

Any velocity coordinates which initially place the beam off the display face are ignored and treated as zero.

E.12.3.6 Comments

The program was written in FORTRAN IV for use on an IBM System/360. The program requires 33,544 bytes of storage.

E.13 CONVERTED STUDY PROGRAMS

E.13.1 Seismic Ray-Tracing Program

E.13.1.1 Purpose

This program calculates the angular range, travel time, and inverse phase speed for both the direct and surface reflected rays, and repeats this calculation for arbitrary equal increments of Snell's constant over any desired range of values.

E.13.1.2 Description

E.13.1.2.1 Input

This program requires a number of layers, N, and for each layer the radii and velocities at upper and lower boundaries. The source position is defined to be at the upper boundary of any layer with the receiver at the surface.

E.13.1.2.2 Computation

This program was written under the LASA Signal Processing Study* and has been converted to System/360 FORTRAN IV.

E.13.1.2.3 Output

For each layer, the velocity gradient and zero-radius velocity are printed along with travel time. Also, angular distance of both direct and reflected ray inverse phase speed, and radius of deepest penetration for each value of Snell's constant is recorded.

E.13.1.3 Program Interaction

Relation of inverse phase speed to range is used in the Inverse Velocity Space Mapping program.

E.13.1.4 Program Restrictions

In its current form, the program is restricted to 95 layers. The source position must be at the upper boundary of one of the 95 layers.

E.13.1.5 Comments

The program is written in FORTRAN IV for the IBM System/360.

E.13.2 Least Squares Wavefront with Range Correction Program

E.13.2.1 Purpose

This program calculates the direction and speed, and thereby the approximate azimuth and range, of the wavefront corresponding to a given set of arrival times at a set of known locations by calculating the best-fitting plane wavefront corresponding to these arrivals. An attempt is made to correct the arrival times for curvature as a function of range.

*IBM Final Report, "LASA Signal Processing Study," Contract No. SD-296, July 15, 1965.

E.13.2.2 Description

E.13.2.2.1 Input

A set of arrival times at a set of known locations is required as input.

E.13.2.2.2 Computation

This program was written under the LASA Signal Processing Study* and has been converted to System/360 FORTRAN IV.

E.13.2.2.3 Output

The program provides azimuth and range to event and the deviation in seconds of the actual arrivals from the best-fitting plane wavefront.

E.13.2.3 Program Interactions

The punched output from this program (deviations of the actual arrivals from the best-fitting plane wavefront) is used as input to the Seismic Steering Delay Anomalies program.

E.13.2.4 Program Restrictions

To determine a plane wavefront, the arrival times at three different locations must be available for the event. The program is arbitrarily restricted to a maximum of 21 subarrays.

E.13.2.5 Comments

This program was written in FORTRAN IV for the IBM System/360.

---

*IBM Final Report, "LASA Signal Processing Study," Contract No. SD-296, July 15, 1965.

E.13.3 Seismic Steering Delay Anomalies Program

E.13.3.1 Purpose

This program calculates the average and standard deviation of the deviation from the best-fitting plane wavefront at each seismometer* from an average for that seismometer, and calculates the loss in db suffered by each wavefront because of mis-steering.

E.13.3.2 Description

E.13.3.2.1 Input

The program accepts deviations in seconds of the actual arrivals from the best-fitting plane wavefront for each wavefront and each seismometer.

E.13.3.2.2 Computation

The average and standard deviation of wave arrival deviations from plane are calculated for each seismometer, along with the loss in db due to mis-steering for each wavefront. The loss is found from

$$\text{Loss} = (10 \log_{10} e)\,(2\pi f\,\sigma)^2$$

where:

σ = the standard deviation

f = the frequency.

E.13.3.2.3 Output

The average arrival time deviations, differences of deviations from average, and db loss are recorded.

---

*Seismometer, as used here, may also be interpreted as the center of a subarray.

E.13.3.3 Program Interaction

This program accepts as card input the deviations of the actual arrivals from the best-fitting plane wavefront from the Least Squares Wavefront program.

E.13.3.4 Program Restrictions

This program arbitrarily limits the number of subarrays to 21 and limits the number of wavefronts to 200. There must be at least three time deviations for each wavefront.

E.13.3.5 Comments

This program was written in FORTRAN IV for the IBM System/360.

E.14 CROSS COVARIANCE OF SEISMIC DATA CHANNELS

E.14.1 Purpose

The program computes and plots the cross-covariance of two seismic data input channels (seismometers or beams).

E.14.2 Description

E.14.2.1 Input

The program accepts digitized data in several formats. Control cards specify the seismometers and segments of information to be processed.

E.14.2.2 Computation

The cross-covariance formulae, where A_i, i = 1,..., n, and B_i, i = 1,..., m, are two sets of data, and $n \leq m$ are:

$$R_j = \left(\sum_{i=1}^{T} A_i \cdot B_{i+j-1} \right) /T - (\text{Average } A \cdot \text{Average } B);\ j = 1,\ldots, m$$

where:

$$T = \text{minimum } (n,\ m - j + 1),$$

$$\text{Average } A = \left(\sum_{i=1}^{n} A_i \right) / n;$$

$$\text{Average } B = \left(\sum_{i=1}^{m} B_i \right) / m;$$

and

$$S_j = \left(\sum_{i=1}^{T} A_{i+j-1} \cdot B_i \right) / T - (\text{Average } A \cdot \text{Average } B);\ j = 1, \ldots, n$$

where:

$$T = n - j + 1.$$

(The above is a modification of the method of J. R. Healy and B. P. Bogert as found in the "System/360 Scientific Subroutine Package Programmer's Manual," IBM Corporation, Form H20-0205.)

E.14.2.3 Output

The output consists of a CALCOMP plotter tape which results in an annotated graph of each seismometer and the cross-covariance curve.

E.14.3 Program Interaction

None.

E.14.4 Program Restrictions

The selected segment of any seismometer cannot be greater than 2400 observations. (This would be two minutes of LASA data if every sample period is considered.)

E.14.5 Comments

The program is written in IBM 7090 FORTRAN IV but could be converted for use on another machine if CALCOMP plotter subroutines were available for that computer.

E.15 POWER SPECTRA

E.15.1 Purpose

The Power Spectra program calculates the Fourier transform of seismometer traces each consisting of N real data samples obtained from a LASA edit tape or tapes. The number of samples is taken to be a power of 2. Fourier transforms are obtained for two seismometer traces at a time. The program will also operate on a single seismometer trace but with some loss in efficiency.

E.15.2 Description

E.15.2.1 Input

Input for the program consists of: (a) an 800 BPI FORTRAN compatible LASA edit tape containing the seismometer traces, and (b) at least one control card specifying two seismometer channel numbers, m for the sample size $N = 2^m$ to be taken from the trace of each seismometer specified, and the number of time samples to be skipped before processing. The second of the two seismometer channel numbers is optional.

E.15.2.2 Computation

Given a set of $N = 2^m$ real data samples $X(j)$, $j = 0, \cdots, N-1$, the program computes the set of N complex coefficients $A(k)$, $k = 0, 1, \cdots, N-1$ of the skewed complex Fourier series:

$$X(j) = \sum_{k=0}^{N-1} A(k)\, W^{jk} \qquad j = 0, 1, \cdots, N-1$$

where:

$$W = \exp\left(\frac{-2\pi i}{N}\right)$$

$$i = \sqrt{-1}$$

The A(k) coefficients are found by the inverse formula

$$A(k) = \frac{1}{N} \sum_{j=0}^{N-1} X(j)\, W^{-jk} \quad k=0, 1 \cdots, N-1$$

The Cooley-Tukey algorithm* is employed in the calculations

E.15.2.3 Output

Output of the program consists of an off-line printout of: (a) the time and channel data appearing in the header record of the LASA edit tape, (b) tabulation of the data samples taken from each seismometer trace, and (c) a tabulation of the complex Fourier series coefficients $A(k)$, $k=0, 1, \cdots, N/2$. Because the data samples are real, the remaining $A(k)$ coefficients are not printed for $A(N-k) = \tilde{A}(k)$ $k=1, 2, \cdots, \frac{N}{2} -1$, where $\tilde{A}(k)$ means the conjugate of $A(k)$.

E.15.3 Program Interaction

None.

E.15.4 Program Restrictions

The sample size taken from a given seismometer trace must be a power of 2 not exceeding $8192 = 2^{13}$ or less than 2.

E.15.5 Comments

The program is written in FORTRAN IV and MAP for the IBM 7090.

*J. W. Cooley and J. W. Tukey, "An Algorithm for the Machine Calculation of Complex Fourier Series," Mathematics of Computation, Vol. 19, April 1965, p 297.

Appendix F

COMMENTS AND RECOMMENDATIONS ON THE IBM LASA STUDY

F.1 INTRODUCTION

This appendix* presents comments on the following topics related to the IBM LASA study and system efforts:

a. Developing the Steering Delays (Section F.2)
b. Consideration of Post-P Arrivals (Section F.3)
c. Processing and Processor Configuration (Section F.4)
d. Array Synthesis (Section F.5)
e. Source Location and Use of Several LASAs (Section F.6)
f. Problems for Further Research (Section F.7)
g. LASA Seismic Handbook (Section F.8).

F.2 DEVELOPING THE STEERING DELAYS

Specification of a first set of beam steering delays to be programmed into the detection processor as soon as it becomes available is perhaps the most urgent task to be undertaken. It is clear that such delays must at first be based essentially on experimental data of seismic wave fronts actually received at LASA.

The current IBM effort to relate the delays to those corresponding to idealized plane wave fronts appears to be a reasonable approach to this problem. This approach has a possible advantage over the standard method using Jeffreys-Bullen travel times with local station corrections in that it separates the problem of obtaining the steering delays from the problem of source location. For each wave front, the steering delays are determined in such a way as to minimize the residuals from an idealized front rather than to conform to a separately computed source location which in any case will often become available only some time after the event.

*This appendix is based on notes by A. F. Gangi, Associate Professor, Department of Geology and Geophysics, MIT, and Consultant to IBM LASA Project.

The present plane wave front approach uses a least squares plane wave front to classify the steering delays according to inverse velocity components (W_x, W_y) and lists the deviations from that plane. There might be an advantage to using a best fitting quadratic wave front instead, so as to permit study of the two wave curvatures. If these curvatures, in addition to the velocities, should be found to behave in a reasonably predictable manner, then the quadratic reference wave fronts would of course permit smaller residuals, and hence, improved steering than the plane wave method.

Initially, all steering delays must be based on an entirely empirical formulation, using experimental delays. Based on plane (or quadratic) wave fronts, the delays must be adjusted for some average value of the residual at each subarray. However, it is very important for several reasons to also begin to base this information on a more exact theoretical foundation in terms of the earth's structure of propagation velocities which in turn defines travel times and phase velocities. This is what in effect has already been done when the Jeffreys-Bullen Tables were constructed. However, with the advent of large array technology, it should become possible to reach into the velocity profile with greater detail and precision, based on wave velocity and curvature measurements as well as travel times.

The most immediate reason why this theoretical basis must be established is to provide a good method for steering to those parts of the earth from which seismic events of adequate strength are relatively scarce. Another reason is that an accurate knowledge of the earth's velocity structure will permit more accurate utilization of later arrivals to identify events and pinpoint their locations and times of origin. Finally, a better knowledge of the earth's structure is of itself of great scientific interest and can in the longer run lead to a more systematic understanding of geophysical questions.

F.3 CONSIDERATION OF POST-P ARRIVALS

Seismic arrivals following the initial P wave will be received, and must, therefore, be identified even if their further analysis will not always be required. In addition, these later arrivals, when grouped and identified, will aid in the

discrimination problem and may improve event location accuracy. Arrivals of importance will be pP, PcP, S, and others. pP and to some extent PcP should be particularly useful in source depth estimation. Amplitude of the various phases should be compared to begin to accumulate information on seismic source radiation patterns in P and S modes. Such patterns may become useful discriminants.

F.4 PROCESSING AND PROCESSOR CONFIGURATION

The necessity for a "post-detection or pre-event" processing function is discussed, although this function might be included in the event processor. The problem is to weed out in a logical manner the many arrivals the detection processor will detect, including post-P and side-lobe detections. The following functions in particular should be considered.

a. Detect and identify pP to obtain an estimate of source depth, if any.

b. Detect and identify PcP to obtain further information on source depth and distance to the source.

c. Detect and identify other arrivals with relatively large amplitudes.

d. Decide which events and which arrivals should be subjected to further processing by the event processor.

Once some of the arrivals have been identified, beams should be formed at correct times and velocities to definitely identify as many of the original detections as practicable and, where necessary, to produce clean wave forms and other required event processor outputs.

If it turns out that event beamforming and event beam selections place an excessive load on beamforming capability, it may be desirable to form successively closer together event beams, always dividing up the remaining area into a few beams and selecting the best one, rather than immediately covering the whole area with many closely spread beams.

A suggestion is made to investigate an adaptive technique using correlation to sharpen an event beam by adaptively adjusting its steering delays.

The Seismic Bulletin to be published should include not only the classical seismic station outputs, but also the noise statistics, the signal phase speeds,

and perhaps the wave front curvatures as measured by the array.

The possibility of improving signal-to-noise ratio by vectorially combining the three outputs of the three-component seismometer should also be investigated.

F.5 ARRAY SYNTHESIS

It may be worthwhile to make an array geometry synthesis program based on the superposition principle. The array patterns of a triangle, square, pentagon, and hexagon should be made. Then, beam patterns of arrays composed of combinations of these simple geometries can be readily calculated by taking into account the scale change on a pattern in wave number space of a change in the array size in physical space. Also, a rotation in physical space corresponds to a rotation in wave number space. This should be a great help in the synthesis of patterns. It is not necessary to limit oneself to the regular polygons in performing this study, and it also is not necessary to synthesize array patterns using just one type of polygon for the whole array.

F.6 SOURCE LOCATION AND USE OF SEVERAL LASAS

The use of more than one LASA can be expected to somewhat improve location accuracy over a single LASA because:

a. One of several LASAs might be in a more advantageous location relative to the event.

b. An improvement of the order of $\sqrt{N}$ when using N LASAs should follow statistically.

c. If four or more LASAs are used, then world-wide base lines for calculating source location become available, greatly improving the location accuracy. However, the same effect can be achieved using single seismometers in place of LASAs except that the signal-to-noise ratio would be lower, and hence, the detection identification and localization threshold would necessarily be at a higher signal level.

F.7 PROBLEMS FOR FURTHER RESEARCH

Some problems which should be investigated by using the LASA are:

a. The velocity distribution in the earth

b. The attenuation of waves in the earth

c. Earthquake statistics

d. Variation of earthquake spectra with magnitude

e. Radiation patterns of earthquakes

f. Microseismic noise statistics

g. Weather or storm location

h. Local geological structure

i. Earthquake prediction.

A better knowledge of the velocity distribution in the earth can be obtained from the measured arrival times, horizontal velocities, and curvatures of the waves incident on the array. This problem is closely related to that of determining the proper steering delays to form beams. In addition, the amplitudes of the waves can also provide information regarding the density distribution in the earth. The variation of the velocity and density distributions with azimuth would delineate the lateral inhomogeneities in the properties of the earth's interior.

From the difference in the spectra of the direct P arrival and later arrivals, some measure of the attenuation in the earth can be obtained. Before these measurements can be made with accuracy, it will be necessary to determine the effects of the local geology and the source radiation patterns on the spectra of the received waves.

With the automatic detection, localization, depth determination, and (to some degree) magnitude determination ability of LASA, along with its sensitivity to small magnitude earthquakes, it should be very easy to obtain very good earthquake statistics in a short time and without the normal drudgery involved in obtaining these statistics. These data are also of value to the operational system to determine some of the operating parameters.

Because the signals received at LASA will be digitized and available on magnetic tape, it will be reasonably simple to obtain the spectra of these signals.

The correlation of the characteristics of these spectra with other earthquake parameters would lead to a better understanding of the earthquake source mechanism.

With a world-wide distribution of LASAs or even with the detection of later arrivals from a single LASA, it should be possible to obtain information on earthquake radiation patterns on a routine basis. This too would lead to a better understanding of the source mechanism of the underlying causes of tectonic activity in the earth.

The study of microseismic noise statistics would lead to a better knowledge of the local geology and its effects on the propagation of microseismic noise. In addition, because microseismic noise is believed to be caused by weather (storms) at sea or near the coasts, this study of the microseisms could be used to locate and track such storms. The information obtained here would also be of value to the operational system.

The local geological structure can be studied by a knowledge of the station corrections at each site and their variations with distance and azimuth. Further information on the local or region structure can be obtained by looking at small, local events such as local quakes or quarry blasts. In this sense, the array can be used as a tool to perform refraction profiles.

Finally, it is possible that LASA can be used as a tool for earthquake prediction. This study would be performed in conjunction with the earthquake statistics studies because it has been indicated that earthquake activity (small events) increase prior to larger events. This theory is not very well substantiated and LASA would be a convenient tool to verify or refute the hypothesis.

F.8 LASA SEISMIC HANDBOOK

Another suggestion is to begin work on a LASA Seismic Handbook in which characteristics of the array are kept. This would include such things as beam patterns, processing gain, signal loss due to timing errors, noise statistics and their temporal (seasonal) variation. Earthquake statistics, maps of seismic regions as determined by LASA and many other kinds of data. It would not be

necessary to explain the given results or to explain how they were obtained. It would suffice to give references to the original papers and reports from which the data were taken. In this way, all the pertinent data of value in the operation of LASA would be at one's fingertips in condensed form.

Appendix G

DOCUMENT CONTROL DATA—R&D (DD1473)

Unclassified
Security Classification

DOCUMENT CONTROL DATA - R&D

(Security classification of title, body of abstract and indexing annotation must be entered when the overall report is classified)

1. ORIGINATING ACTIVITY (Corporate author) Federal Systems Division International Business Machines Corporation Gaithersburg, Maryland	2a. REPORT SECURITY CLASSIFICATION Unclassified 2b GROUP

3. REPORT TITLE

LASA Signal Processing, Simulation, and Communications Study

4. DESCRIPTIVE NOTES (Type of report and inclusive dates)

Second Quarterly Technical Report May - August 1966

5. AUTHOR(S) (Last name, first name, initial)

Not Applicable

6. REPORT DATE	7a. TOTAL NO. OF PAGES	7b. NO. OF REFS
May - August 1966	127	6

8a. CONTRACT OR GRANT NO. AF 19(628)-5948 b. PROJECT NO. c. ARPA Order No. 800 d.	9a. ORIGINATOR'S REPORT NUMBER(S) None 9b. OTHER REPORT NO(S) (Any other numbers that may be assigned this report) Not Applicable

10. AVAILABILITY/LIMITATION NOTICES

Distribution of this report is unlimited.

11. SUPPLEMENTARY NOTES	12. SPONSORING MILITARY ACTIVITY
None	Advanced Research Projects Agency Washington, D. C.

13. ABSTRACT

In the First Quarterly Technical Report, 14 May 1966, a functional system description of a LASA Signal Processing System was hypothesized. Certain system parameters were outlined and bounded to permit a definition of the signal processing concept. This, the Second Quarterly Technical Report, discusses important system parameters in greater detail to provide further technical support to the system concept and describes some of the supporting efforts.

Sections 1 and 2 describe the work accomplished and plans, respectively. Appendices A to C contain factual detail in the areas of beam analysis, signal processing and processing systems. Appendix D describes effort relating to communications instrumentation. A summary description of the programs currently under development is given in Appendix E. Overall program comments and recommendations on relevant topics of seismological interest are presented in Appendix F.

DD FORM 1 JAN 64 1473

Unclassified
Security Classification

14. KEY WORDS	LINK A		LINK B		LINK C	
	ROLE	WT	ROLE	WT	ROLE	WT
Signal Processing						
Seismic						
LASA						

INSTRUCTIONS

1. ORIGINATING ACTIVITY: Enter the name and address of the contractor, subcontractor, grantee, Department of Defense activity or other organization *(corporate author)* issuing the report.

2*a*. REPORT SECURITY CLASSIFICATION: Enter the overall security classification of the report. Indicate whether "Restricted Data" is included. Marking is to be in accordance with appropriate security regulations.

2*b*. GROUP: Automatic downgrading is specified in DoD Directive 5200.10 and Armed Forces Industrial Manual. Enter the group number. Also, when applicable, show that optional markings have been used for Group 3 and Group 4 as authorized.

3. REPORT TITLE: Enter the complete report title in all capital letters. Titles in all cases should be unclassified. If a meaningful title cannot be selected without classification, show title classification in all capitals in parenthesis immediately following the title.

4. DESCRIPTIVE NOTES: If appropriate, enter the type of report, e.g., interim, progress, summary, annual, or final. Give the inclusive dates when a specific reporting period is covered.

5. AUTHOR(S): Enter the name(s) of author(s) as shown on or in the report. Enter last name, first name, middle initial. If military, show rank and branch of service. The name of the principal author is an absolute minimum requirement.

6. REPORT DATE: Enter the date of the report as day, month, year; or month, year. If more than one date appears on the report, use date of publication.

7*a*. TOTAL NUMBER OF PAGES: The total page count should follow normal pagination procedures, i.e., enter the number of pages containing information.

7*b*. NUMBER OF REFERENCES: Enter the total number of references cited in the report.

8*a*. CONTRACT OR GRANT NUMBER: If appropriate, enter the applicable number of the contract or grant under which the report was written.

8*b*, 8*c*, & 8*d*. PROJECT NUMBER: Enter the appropriate military department identification, such as project number, subproject number, system numbers, task number, etc.

9*a*. ORIGINATOR'S REPORT NUMBER(S): Enter the official report number by which the document will be identified and controlled by the originating activity. This number must be unique to this report.

9*b*. OTHER REPORT NUMBER(S): If the report has been assigned any other report numbers *(either by the originator or by the sponsor)*, also enter this number(s).

10. AVAILABILITY/LIMITATION NOTICES: Enter any limitations on further dissemination of the report, other than those imposed by security classification, using standard statements such as:

(1) "Qualified requesters may obtain copies of this report from DDC."

(2) "Foreign announcement and dissemination of this report by DDC is not authorized."

(3) "U. S. Government agencies may obtain copies of this report directly from DDC. Other qualified DDC users shall request through ____________."

(4) "U. S. military agencies may obtain copies of this report directly from DDC. Other qualified users shall request through ____________."

(5) "All distribution of this report is controlled. Qualified DDC users shall request through ____________."

If the report has been furnished to the Office of Technical Services, Department of Commerce, for sale to the public, indicate this fact and enter the price, if known.

11. SUPPLEMENTARY NOTES: Use for additional explanatory notes.

12. SPONSORING MILITARY ACTIVITY: Enter the name of the departmental project office or laboratory sponsoring *(paying for)* the research and development. Include address.

13. ABSTRACT: Enter an abstract giving a brief and factual summary of the document indicative of the report, even though it may also appear elsewhere in the body of the technical report. If additional space is required, a continuation sheet shall be attached.

It is highly desirable that the abstract of classified reports be unclassified. Each paragraph of the abstract shall end with an indication of the military security classification of the information in the paragraph, represented as *(TS)*, *(S)*, *(C)*, or *(U)*.

There is no limitation on the length of the abstract. However, the suggested length is from 150 to 225 words.

14. KEY WORDS: Key words are technically meaningful terms or short phrases that characterize a report and may be used as index entries for cataloging the report. Key words must be selected so that no security classification is required. Identifiers, such as equipment model designation, trade name, military project code name, geographic location, may be used as key words but will be followed by an indication of technical context. The assignment of links, rules, and weights is optional.

IBM®